Supporting Information for

A Robust Heterodimeric Bis-Rh(III)-Porphyrin Macrocycle for the Self-Assembly of a Kinetically Stable [2]-Rotaxane

Naoyuki Hisano[a,†,*], Virginia Valderrey[a], Gemma Aragay and Pablo Ballester[a,b*]

[a] *Institute of Chemical Research of Catalonia (ICIQ), The Barcelona Institute of Science and Technology (BIST), Avgda. Països Catalans, 16, 43007 Tarragona, Spain.*

†Current address: Naoyuki Hisano, Graduate School of Advanced Science and Engineering, Hiroshima University, 1-3-1 Kagamiyama, Higashi-Hiroshima, Hiroshima 739-8562, Japan.

[b] *ICREA, Passeig Lluís Companys, 23, 08010 Barcelona, Spain.*

*Correspondence to: Naoyuki Hisano chemhisano@hiroshima-u.ac.jp and Pablo Ballester pballester@iciq.es.

Contents

1. General information and instruments

^{1}H and ^{13}C NMR spectra were recorded on a Bruker Avance 300, Bruker Avance 400, Bruker Avance 500, or Bruker Avance 500 with cryoprobe, and chemical shifts were reported on the delta scale in ppm relative to residual chloroform (δ = 7.26 and 77.2 for ^{1}H and ^{13}C, respectively), pyridine (δ = 8.74 and 150.4 for ^{1}H and ^{13}C, respectively), and 1,1,2,2-tetrachloroethane (δ = 6.00 and 73.8 for ^{1}H and ^{13}C, respectively). High Resolution Mass Spectra (HRMS) were obtained on a Bruker HPLC-ESI-TOF (MicroTOF Focus), Bruker HPLC-ESI-QqTOF (MaXis Impact) or Thermo Fisher Scientific Q Exactive Orbitrap equipped with a Heated Electrospray Ionization (HESI) source. Melting points (Mp) were measured with a MP70 Melting Point System. Preparative separations were performed by silica gel gravity column chromatography (silica gel 60 Å and 230–400 mesh particle size. The size-exclusion chromatography was performed using Agilent PLgel 3μm GPC column. Dichloromethane was used as the eluting solvent. Commercially available reagents and solvents were used without purification except where noted.

2. Experimental Procedures

Synthesis of free-base bis-porphyrin ***1-H₂***.

To a solution of 4-(10,15,20-tris(4-pentylphenyl)porphyrin-5-yl)aniline (590 mg, 0.70 mmol) and 4-(benzyloxy)pyridine-2,6-dicarbonyl dichloride (99 mg, 0.32 mmol) in THF (16 mL) were added pyridine (0.1 mL) and 4-(dimethylamino)pyridine (280 mg, 2.29 mmol) under argon. After the mixture was stirred at room temperature for 16 h, the reaction mixture was poured into saturated $NaHCO_3$ solution, and the aqueous layer was extracted with CH_2Cl_2. The organic layer was washed with brine, dried over sodium sulfate, and concentrated under reduced pressure. The residue was purified by silica-gel column chromatography (50%-100% CH_2Cl_2/hexane) and biobeads to give a purple solid (543 mg, 89%). Mp: > 300 °C. ^{1}H NMR (chloroform-*d*, 400 MHz): δ 10.04 (s, 2H), 8.80-8.93 (m, 16H), 8.32 (d, 4H, J = 8.4 Hz), 8.29 (s, 2H), 8.25 (d, 4H, J = 8.4 Hz), 8.10 (d, 8H, J = 7.8 Hz), 7.54 (d, 4H, J = 8.4 Hz), 7.40-7.60 (m, 5H), 5.45 (s, 2H), 2.87-3.01 (m, 12H), 1.84-1.97 (m, 12H), 1.42-1.55 (m, 24H), 1.02 (t, 6H, J = 7.0 Hz), 1.00 (t, 12H, J = 7.0 Hz), –2.76 (s, 4H). ^{13}C{^{1}H} NMR (chloroform-*d*, 125 MHz): δ 168.4, 161.6, 151.4, 142.5, 139.6, 139.6, 139.3, 137.0, 135.6, 135.0, 134.8, 134.7, 131.3, 129.1, 129.0, 127.9, 126.2, 120.6, 120.5, 119.1, 118.6, 112.6, 71.2, 36.1, 36.1, 32.0, 31.5, 31.5, 22.9, 22.9, 14.4, 14.3.

Synthesis of diiodo Rh(III) bis-porphyrin ***1-(RhI)₂***.

A solution of $[Rh(CO)_2Cl]_2$ (44.6 mg, 0.115 mmol) in dry CH_2Cl_2 (6 mL) was added dropwise under argon to a mixture of free-base bis-porphyrin **1-H₂** (105 mg, 0.0546 mmol) and anhydrous NaOAc (89.2 mg, 1.09 mmol) in dry CH_2Cl_2 (15 mL). After the resulting reaction mixture was stirred for 3 hours at room temperature under argon in the dark, iodine (83.2 mg, 0.328 mmol) was added, and the mixture was stirred 8 hours at room temperature under argon. The reaction mixture was partially evaporated and passed through alumina (5% THF/CH_2Cl_2), and the organic solution was washed with aqueous KI, water, and then brine, dried over Na_2SO_4, and concentrated under reduced pressure. The desired product was obtained as a purple solid (127 mg, 98%). Mp: > 300 °C. ^{1}H NMR (pyridine-d_5, 400 MHz): δ 11.89 (s, 2H), 9.26 (d, 4H, J = 5.0 Hz), 9.22 (s, 8H), 9.22 (d, 4H, J = 5.0 Hz), 8.80 (dd, 2H, J = 8.4, 2.4 Hz), 8.57 (s, 2H), 8.55 (dd, 2H, J = 8.4, 2.4 Hz), 8.38 (dd, 2H, J = 8.2, 2.1 Hz), 8.34 (dd, 2H, J = 8.2, 2.1 Hz), 8.24-8.32 (m, 12H), 7.69 (d, 2H, J = 7.4 Hz), 7.63 (d, 6H, J = 7.7 Hz), 7.59 (d, 6H, J = 7.7 Hz), 7.54 (t, 2H, J = 7.4 Hz), 7.45 (t, 1H, J = 7.4 Hz), 5.44 (s, 2H), 2.89 (t, 12H, J = 7.6 Hz), 1.78-1.87 (m, 12H), 1.38-1.49 (m, 24H), 0.97 (t, 6H, J = 7.2 Hz), 0.96 (t, 12H, J = 7.2 Hz). ^{13}C{^{1}H} NMR (pyridine-d_5, 125 MHz): δ 168.6, 163.4, 153.1, 150.8, 150.7, 149.9, 144.1, 144.1, 144.1, 144.0, 143.3, 140.2, 139.4, 138.9, 136.7, 136.5, 136.4, 136.2, 136.0, 135.7, 135.5, 135.4, 135.1, 133.7, 133.6, 133.5, 129.7, 129.4, 129.0, 127.9, 127.6, 124.4, 124.3, 123.6, 123.1, 123.1, 122.5, 120.6, 120.4, 113.2, 71.5, 36.6, 32.4, 32.0, 23.4, 14.8. HRMS (ESI$^+$) m/z: $[M+Na]^+$ Calcd for $C_{132}H_{125}I_2O_3N_{11}Rh_2Na$ 2394.6058. Found, 2394.6028.

Synthesis of bis-pyridyl ligand ***2***.

To a solution of 3,5-dimethylpyridin-4-amine (360 mg, 2.95 mmol) and 4-(benzyloxy)pyridine-2,6-dicarbonyl dichloride (409 mg, 1.32 mmol) in dry CH_2Cl_2 was added N,N-diisopropylethylamine (0.5 mL) under argon. After the mixture was stirred at room temperature 16 hours, the reaction mixture was extracted with CH_2Cl_2. The organic

layer was washed saturated $NaHCO_3$ solution and brine, dried over Na_2SO_4, and concentrated under reduced pressure. The solid residue was recrystallized in CH_2Cl_2/EtOAc to give a white solid (304 mg, 48%). Mp: 257-259 °C. ^{1}H NMR (chloroform-*d*, 400 MHz): δ 9.25 (s, 2H), 8.37 (s, 4H), 8.10 (s, 2H), 7.35-7.50 (m, 5H), 5.32 (s, 2H), 2.29 (s, 12H). $^{13}C\{^1H\}$ NMR (chloroform-*d*, 125 MHz): δ 168.2, 161.3, 150.6, 149.6, 142.0, 134.9, 130.2, 129.1, 129.0, 127.9, 112.9, 71.2, 15.7. MS (ESI^+) m/z: $[M+H]^+$ Calcd for $C_{28}H_{28}O_3N_5$ 482.21. Found 482.2.

Macrocycle ***[1-(RhI)$_2$•2]*****:** ^{1}H NMR (1,1,2,2-tetrachloroethane-d_2, 400 MHz): δ 10.47 (s, 2H), 8.96 (d, 2H, *J* = 8.2 Hz), 8.95 (d, 4H, *J* = 5.3 Hz), 8.88-8.91 (m, 8H) 8.87 (d, 4H, *J* = 5.3 Hz), 8.58 (d, 2H, *J* = 5.3 Hz), 8.22 (s, 2H), 8.21 (d, 4H, *J* = 7.6 Hz), 8.13 (d, 2H, *J* = 7.6 Hz), 8.06 (d, 2H, *J* = 7.6 Hz), 8.04 (d, 4H, *J* = 7.6 Hz), 7.93 (d, 2H, *J* = 8.2 Hz), 7.45-7.65 (m, 17H), 7.36 (d, 2H, *J* = 8.2 Hz), 7.34 (s, 2H), 7.27 (s, 2H), 7.07-7.25 (m, 5H), 5.47 (s, 2H), 4.85 (s, 2H), 2.99 (t, 8H, *J* = 7.4 Hz), 2.92 (t, 8H, *J* = 7.4 Hz), 1.82-2.03 (m, 12H), 1.42-1.57 (m, 24H), 1.05 (t, 12H, *J* = 7.0 Hz), 1.01 (t, 6H, *J* = 7.0 Hz), 0.62 (s, 4H), 0.53 (s, 12H).

Synthesis of dichloro Rh(III) bis-porphyrin ***1-(RhCl)$_2$.***

A solution of $[Rh(CO)_2Cl]_2$ (46.5 mg, 0.12 mmol) in toluene (15 mL) was added under argon to a solution of free-base bis-porphyrin **1-H$_2$** (112 mg, 0.06 mmol) in toluene (10 mL). After the resulting reaction mixture was stirred for at 80 °C 14 hours under argon in the dark. The reaction mixture was evaporated and purified by preparative TLC (7% CH_3CN/toluene). The desired product was obtained as a purple solid (100 mg, 80%). Mp: > 300 °C. ^{1}H NMR (pyridine-d_5, 300 MHz): δ 11.40 (s, 2H), 9.18 (m, 16H), 8.54 (br m, 3H), 8.23 (br m, 16H), 7.55 (br m, 20H), 5.40 (s, 2H), 2.84 (m, 12H), 1.78 (m, 12H), 1.39 (m, 24H), 0.91 (m, 18H).

3. Binding studies involving bisporphyrin 1-$(RhI)_2$ and bis-pyridine 2

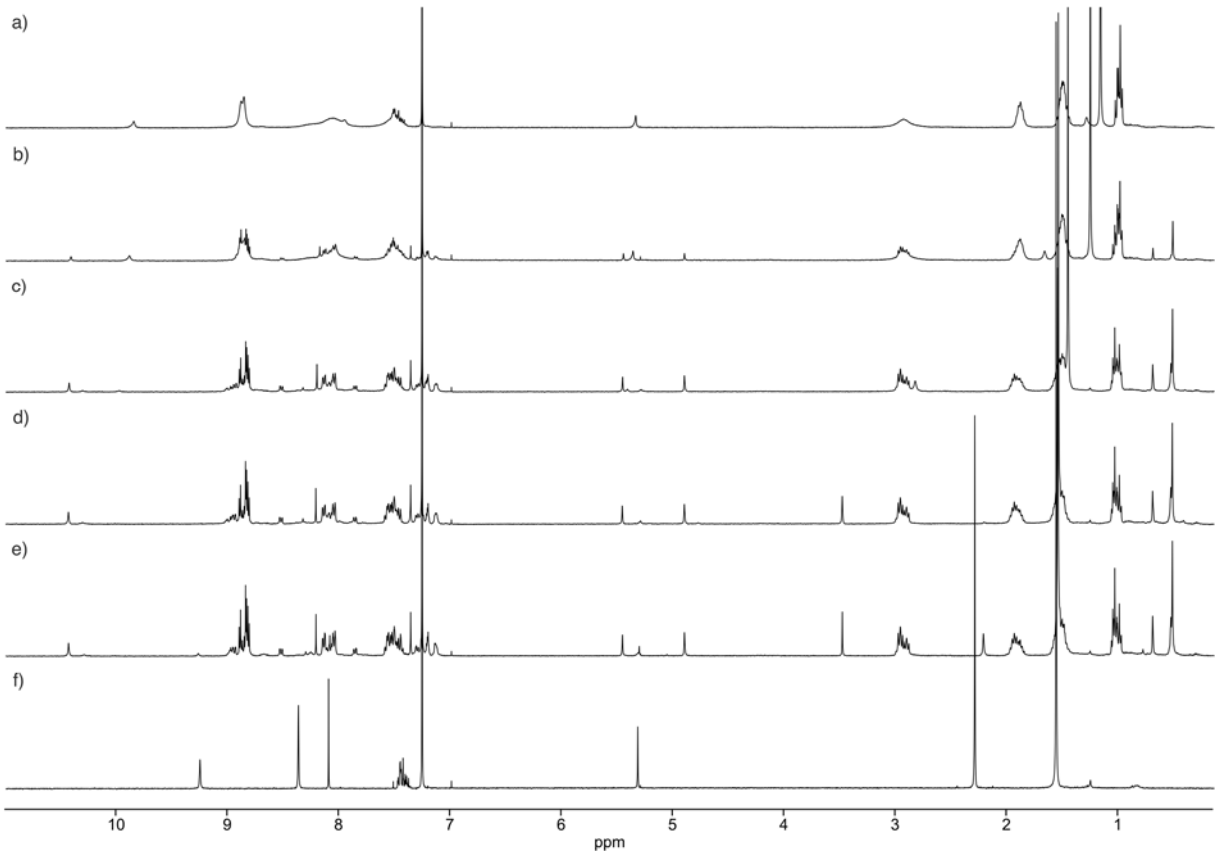

Figure S1. Change of ^{1}H NMR spectra of (a) **1-$(RhI)_2$** (2.0×10^{-3} mol L^{-1}), (b) **1-$(RhI)_2$** with 0.25 equiv. of **2**, (c) **1-$(RhI)_2$** with 0.75 equiv. of **2**, (d) **1-$(RhI)_2$** with 1.0 equiv. of **2**, (e) **1-$(RhI)_2$** with 1.25 equiv. of **2,** and (f) **2** (2.0×10^{-3} mol L^{-1}) in chloroform-*d*.

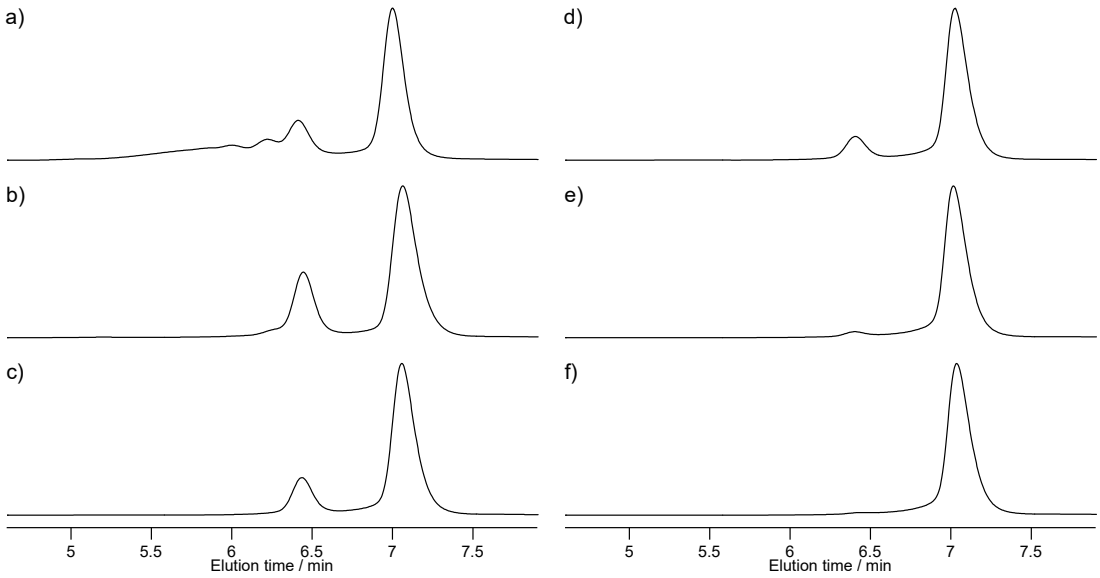

Figure S2. GPC chromatograms of a mixture of **1-(RhI)$_2$** and **2** (a) at initial state and after standing at room temperature for (b) 1 h, (c) 10 h, (d) 1 day, (e) 3 days, and (f) 7days in 1,1,2,2-tetrachloroethane-d_2.

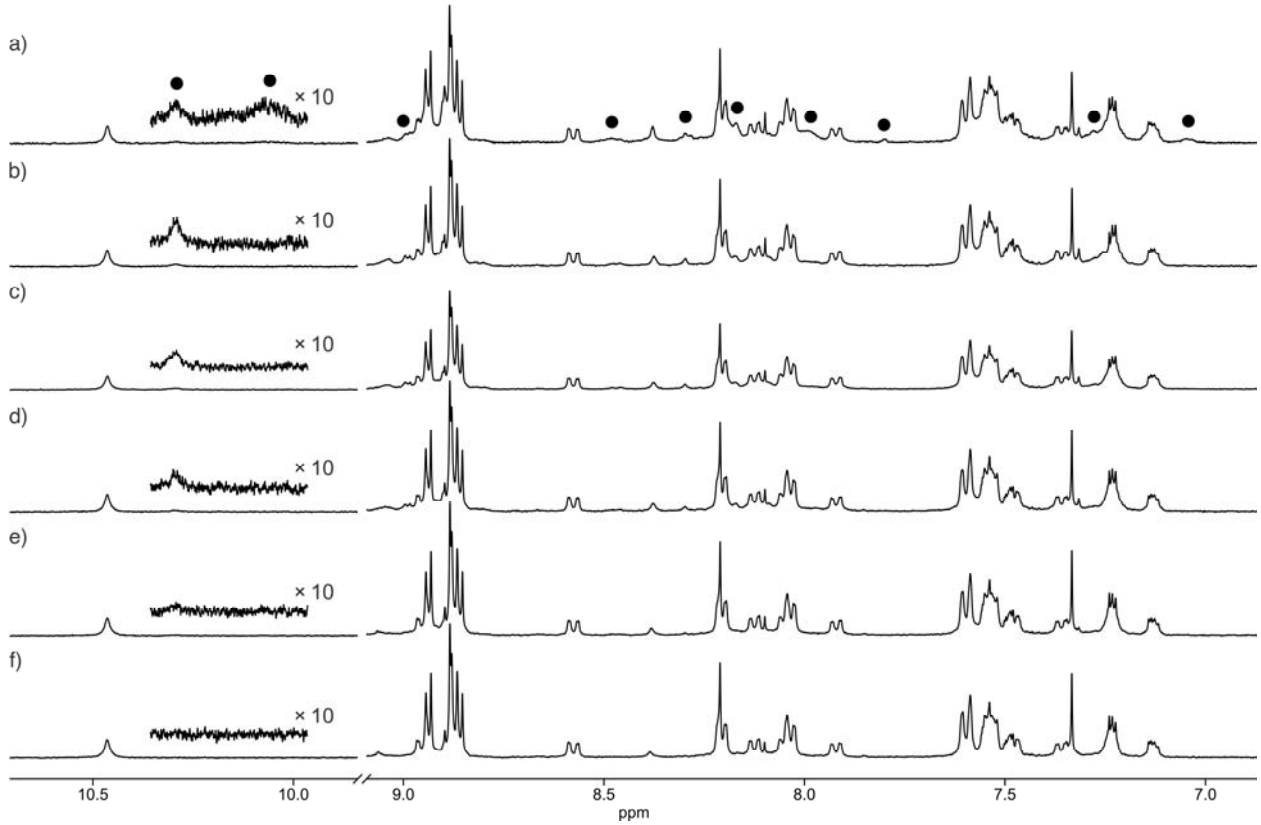

Figure S3. Selected region of the ^{1}H NMR spectra of a 1:1 mixture of **1-(RhI)$_2$** and **2** (a) at initial state and after standing at room temperature for (b) 3 h, (c) 11 h, (d) 1 day, (e) 3 days, and (f) 7 days in 1,1,2,2-tetrachloroethane-d_2. The filled circles denote unassigned oligomeric species.

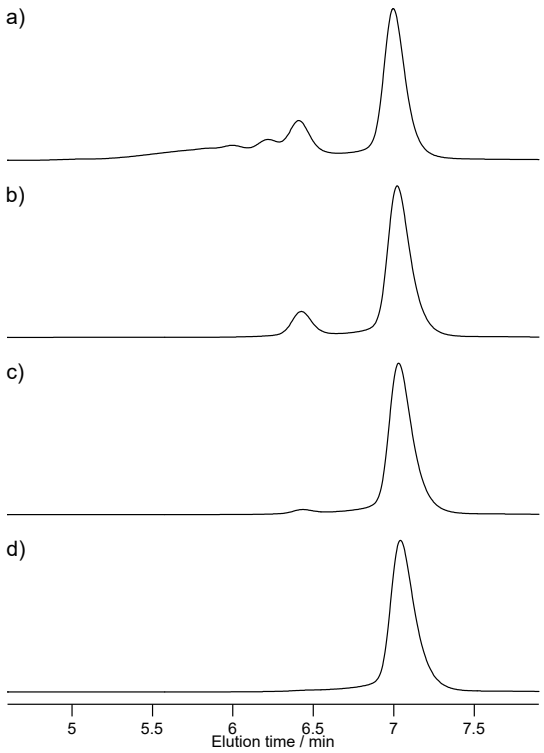

Figure S4. GPC chromatograms of a mixture of **1-(RhI)$_2$** and **2** (a) at initial state and after heating at 80 °C for (b) 1 min, (c) 3 min, and (d) 6 min in 1,1,2,2-tetrachloroethane-d_2.

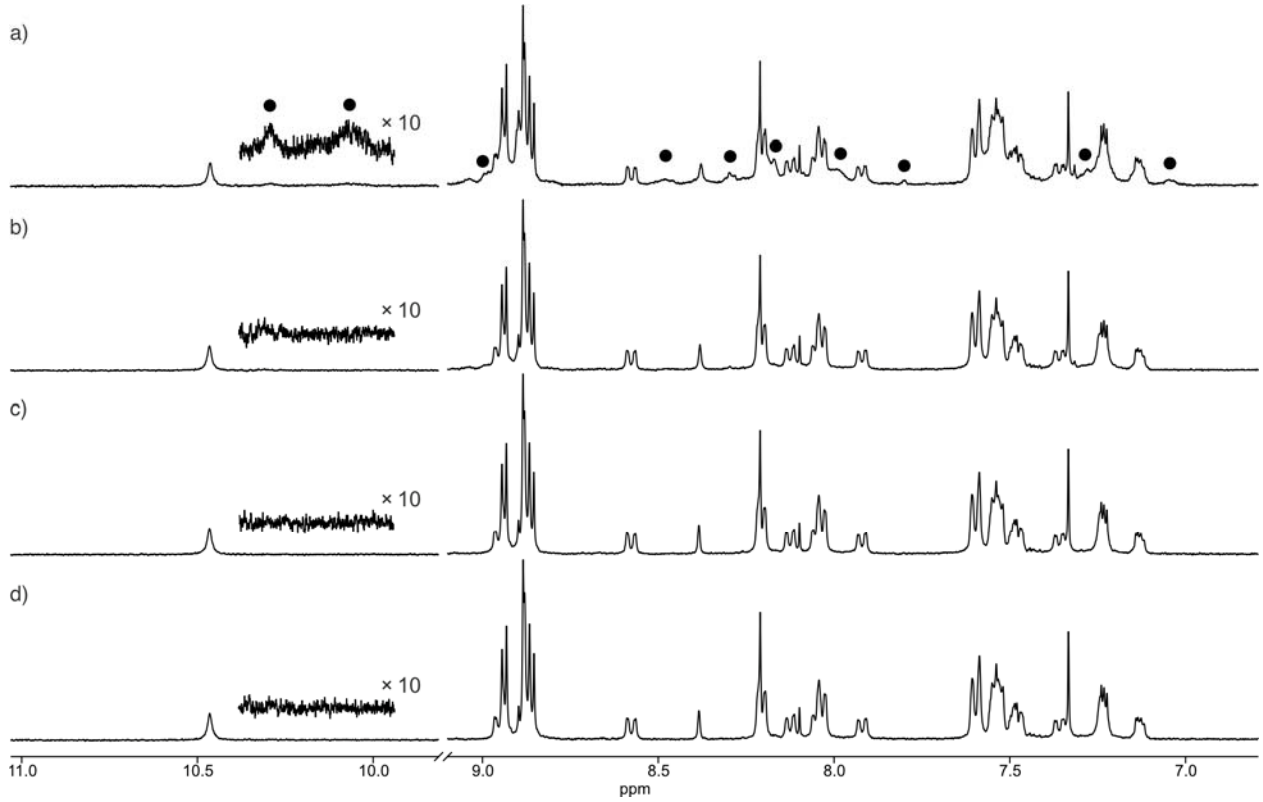

Figure S5. Selected region of the ^{1}H NMR spectra of a 1:1 mixture of **1-(RhI)$_2$** and **2** (a) at initial state and after heating at 80 °C for (b) 1 min, (c) 3 min, and (d) 6 min in 1,1,2,2-tetrachloroethane-d_2. The filled circles denote unassigned oligomeric species.

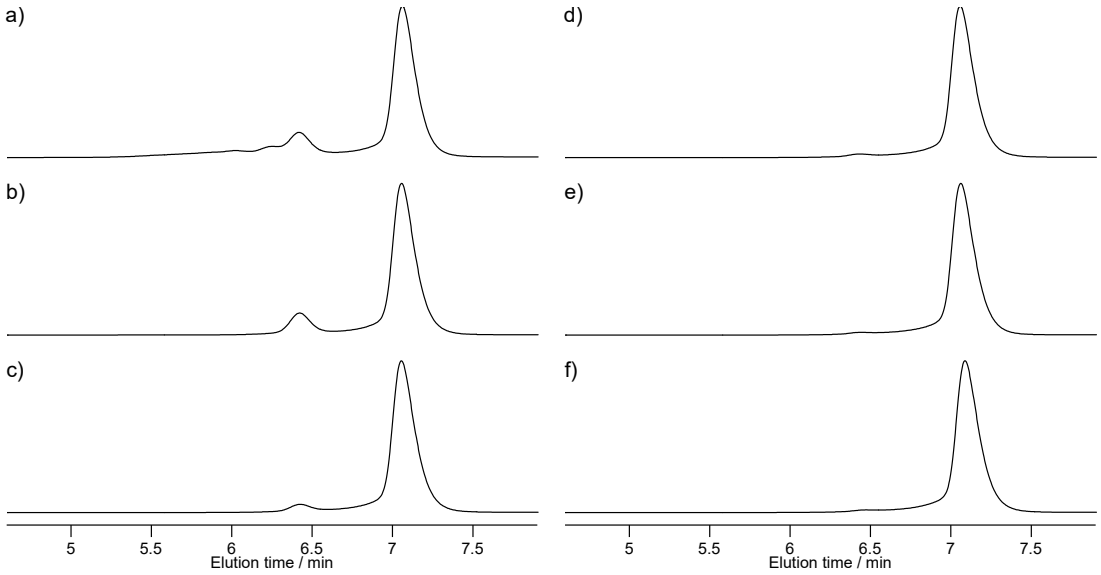

Figure S6. GPC chromatograms of a mixture of **1-(RhI)$_2$** and **2** (a) at initial state and after heating at 80 °C for (b) 1 min, (c) 3 min, (d) 6 min, (e) 10 min, and (f) 30 min in 1,2-dichloroethane.

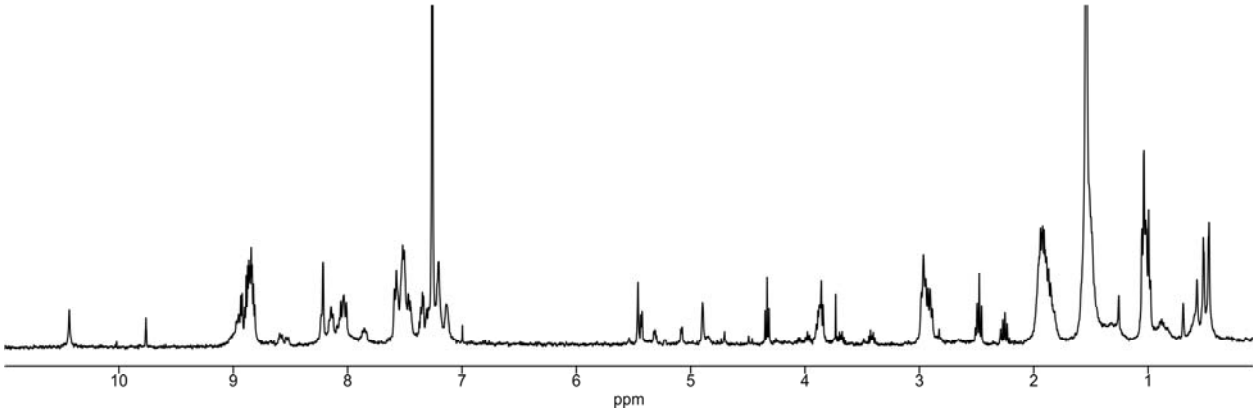

Figure S7. ^{1}H NMR spectra (chloroform-d_1) of a mixture of **1-(RhI)$_2$** and **2** after heating at 80 °C for 18h in 1,2-dichloroethane.

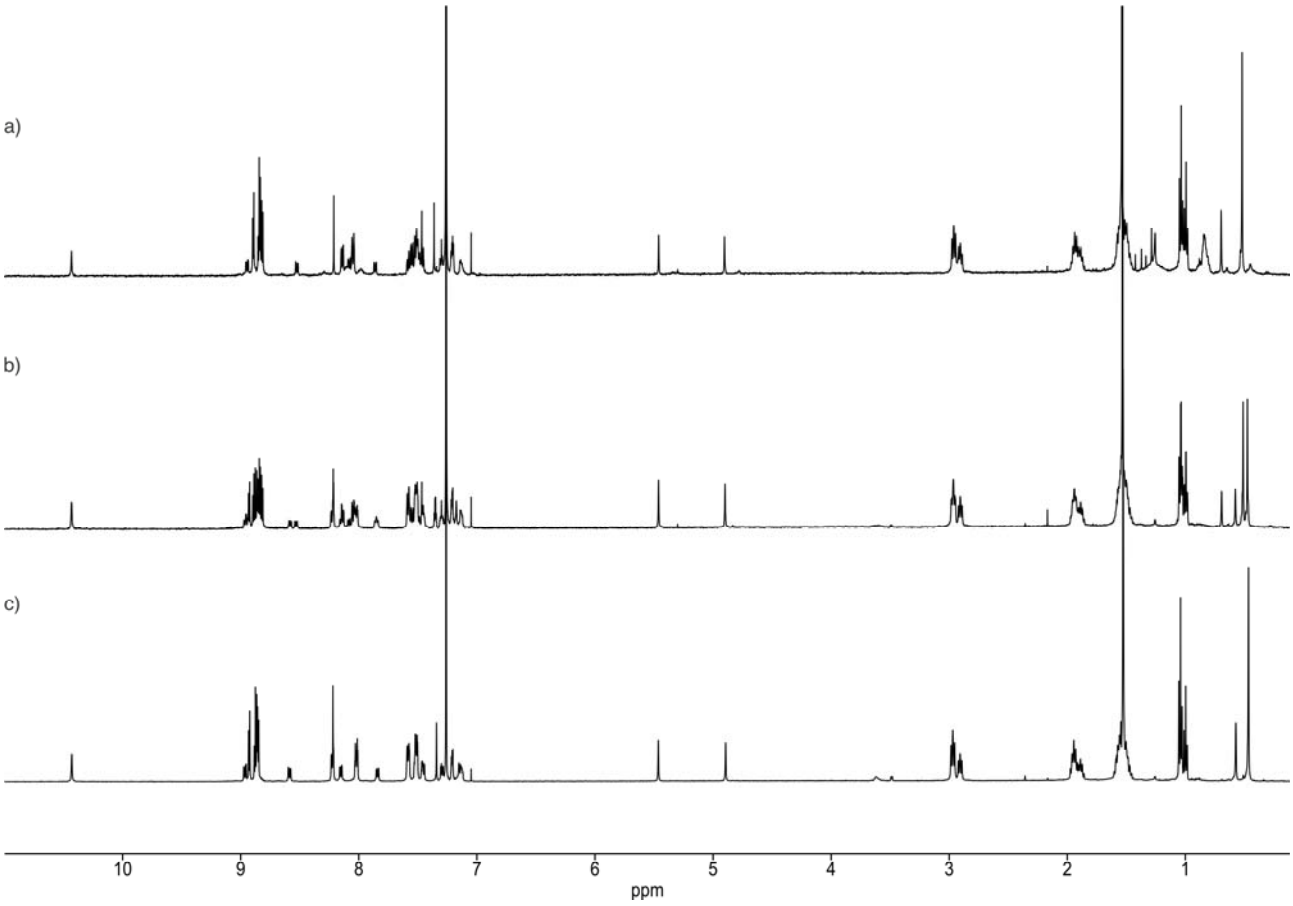

Figure S8 ^{1}H NMR spectra of the three fractions isolated by GPC from the reaction crude of the self-assembly of **1-(RhI)$_2$** and **2** after heating at 80 °C for 18h in 1,2-dichloroethane: (a) fraction 1 corresponds to **1-(RhI)$_2$•2**, (b) fraction 2 corresponds to **1-(RhI)(RhCl)•2**, and (c) fraction 3 corresponds to **1-(RhCl)$_2$•2**.

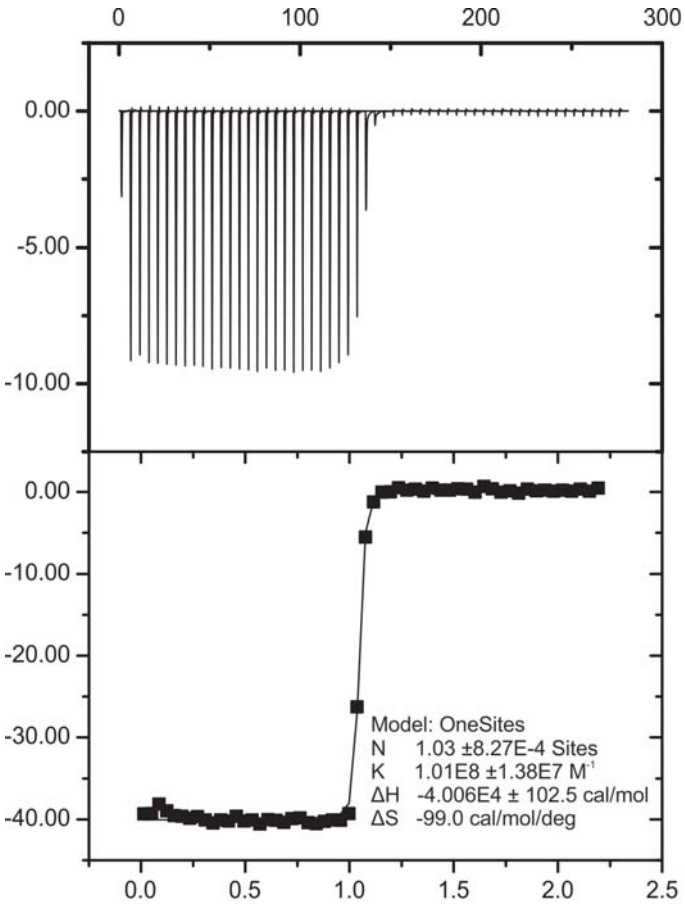

Figure S9. ITC data for the titration of bisporphyrin **1-(RhI)$_2$** (0.1 mM) with bispyridine **2** (1 mM) in chloroform at 298 K. Top) ITC raw data (heat vs. time). Bottom) Integrated data fitted to a theoretical binding isotherm (solid line) for a 1:1 binding model. The formation of oligomers is not considered in the binding model.

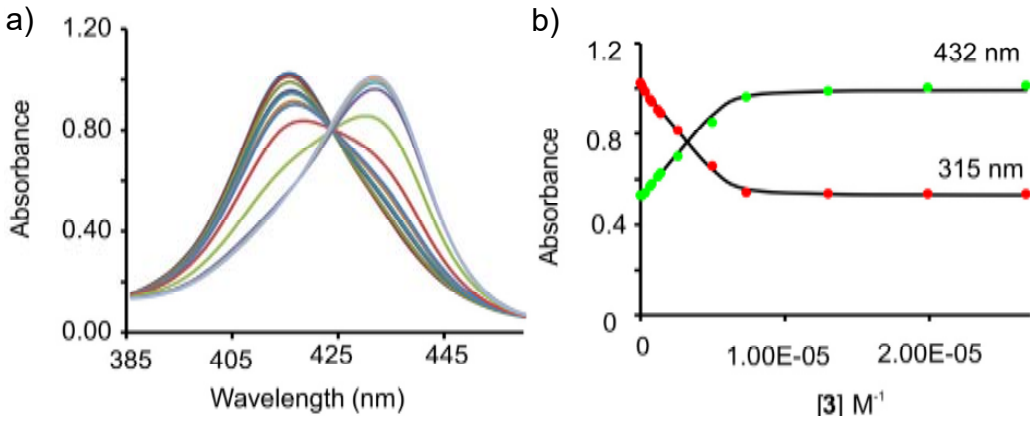

Figure S10. (a) UV/vis absorption spectra of **1-(RhI)$_2$** (4.3×10^{-6} mol L^{-1}) with **2** at 298 K. (b) Fit of the titration data at selected wavelength to a theoretical 1:1 binding model. The formation of oligomers is not considered in the binding model.

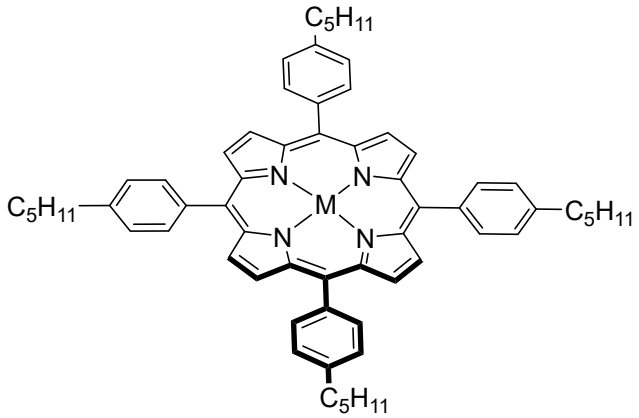

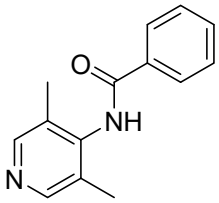

Py-mono

M = Zn(II); Zn(II)-mono
M = Rh(III)-I; Rh(III)-mono

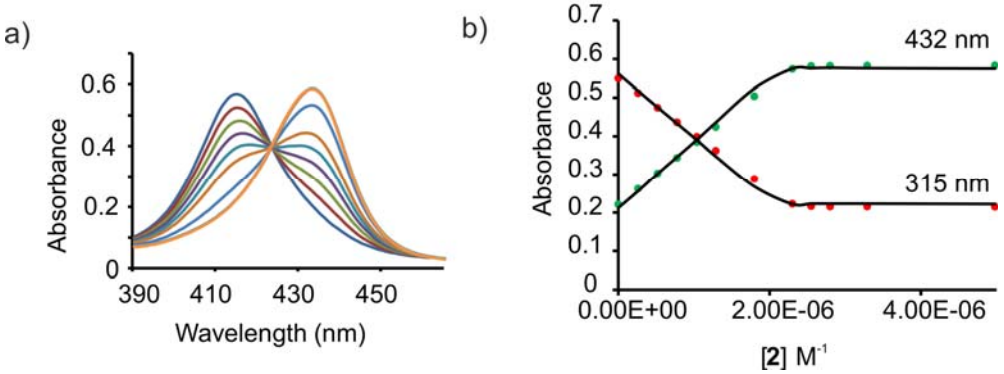

Figure S11. Top) Molecular structure of Rh(III) and Zn(II) monoporphyrins and pyridine ligand used to estimate the strength of the monotopic M-N_{py} interaction (K_m). Bottom) a) UV/vis absorption spectra of monoporphyrin **Rh(III)-mono** with **Py-mono** at 298 K. The concentration of the porphyrin was maintained constant throughout the titration (4.0 x 10^{-6} M in a 10 mm path cell). (b) Fit of the titration data at selected wavelength to a theoretical 1:1 binding model. K_m (Zn(II)-mono•Py-mono) = 5.6×10^3 M^{-1}; K_m (Rh(III)-mono•Py-mono) > 10^7 M^{-1}.

4. HRMS characterization

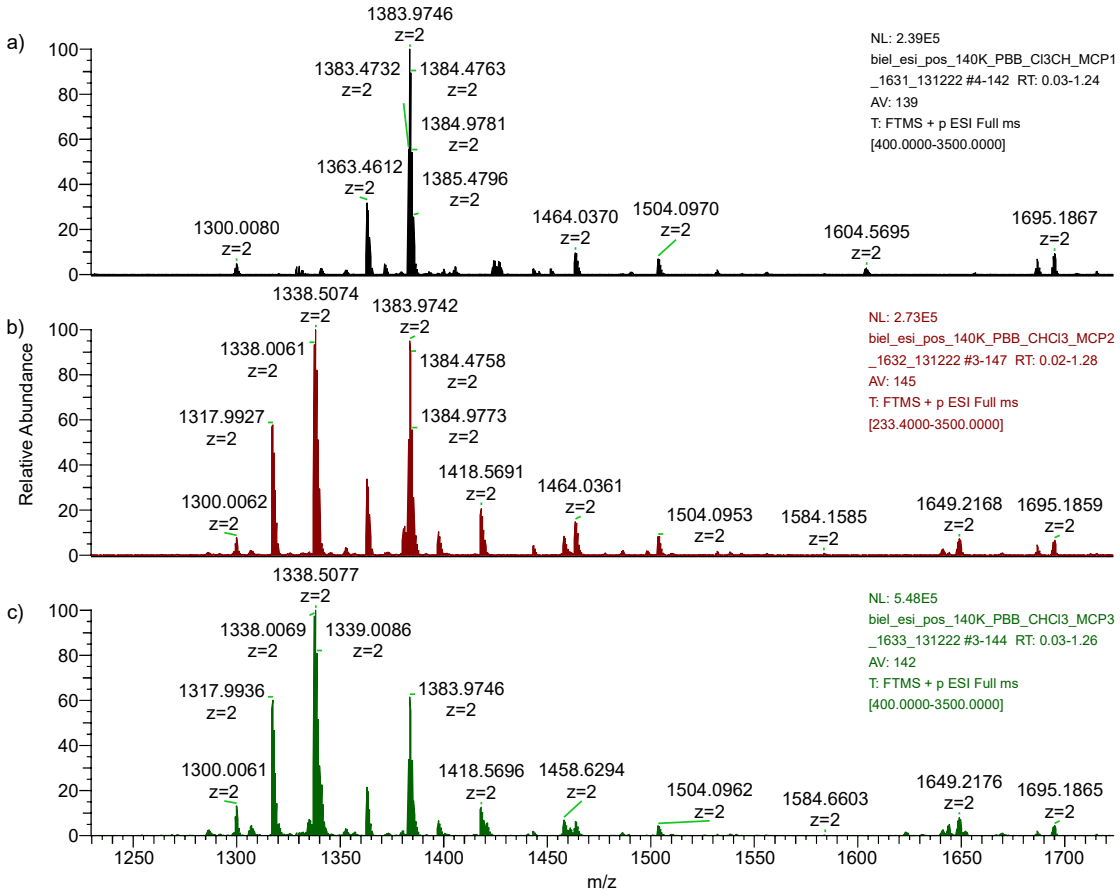

Figure S12. HRMS (ESI^+) spectra of the different fractions isolated by GPC: (a) fraction 1 corresponds to **1-(RhI)$_2$•2**, (b) fraction 2 corresponds to **1-(RhI)(RhCl)•2**, and (c) fraction 3 corresponds to **1-(RhCl)$_2$•2**.

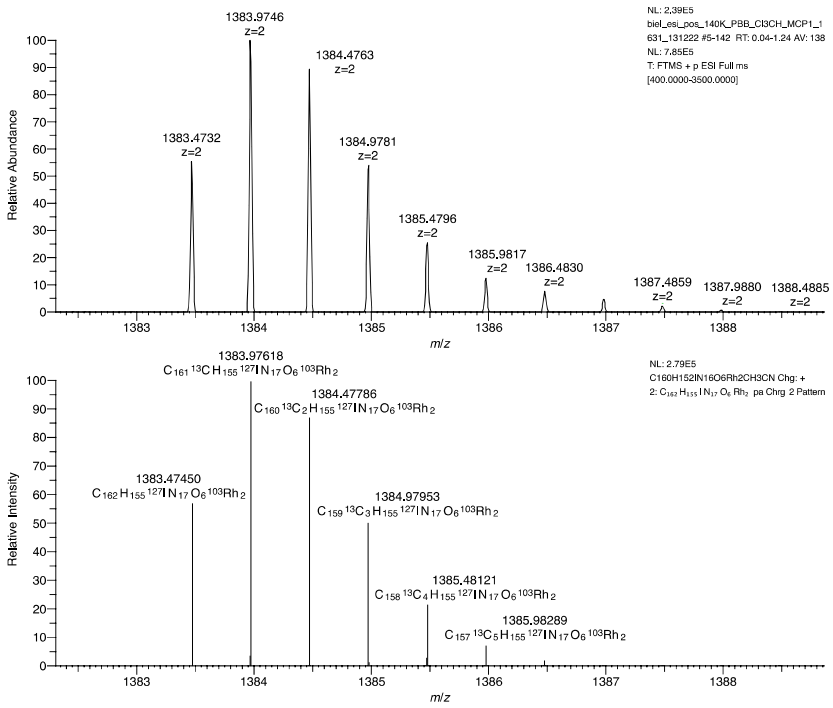

Figure S13. Experimental (top) and simulated (down) isotopic distribution of ion peak $[M\text{-}I+CH_3CN]^{2+}$ (M = **1-(RhI)$_2$•2**).

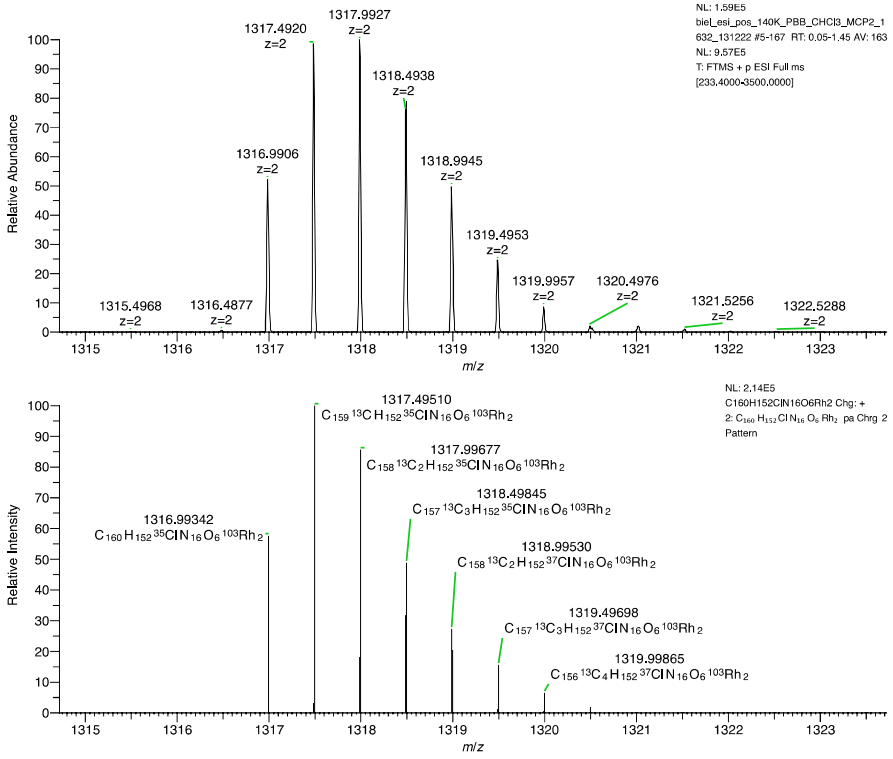

Figure S14. Experimental (top) and simulated (down) isotopic distribution of ion peak $[M\text{-}I]^{2+}$ (M = **1-(RhI)(RhCl)•2**.

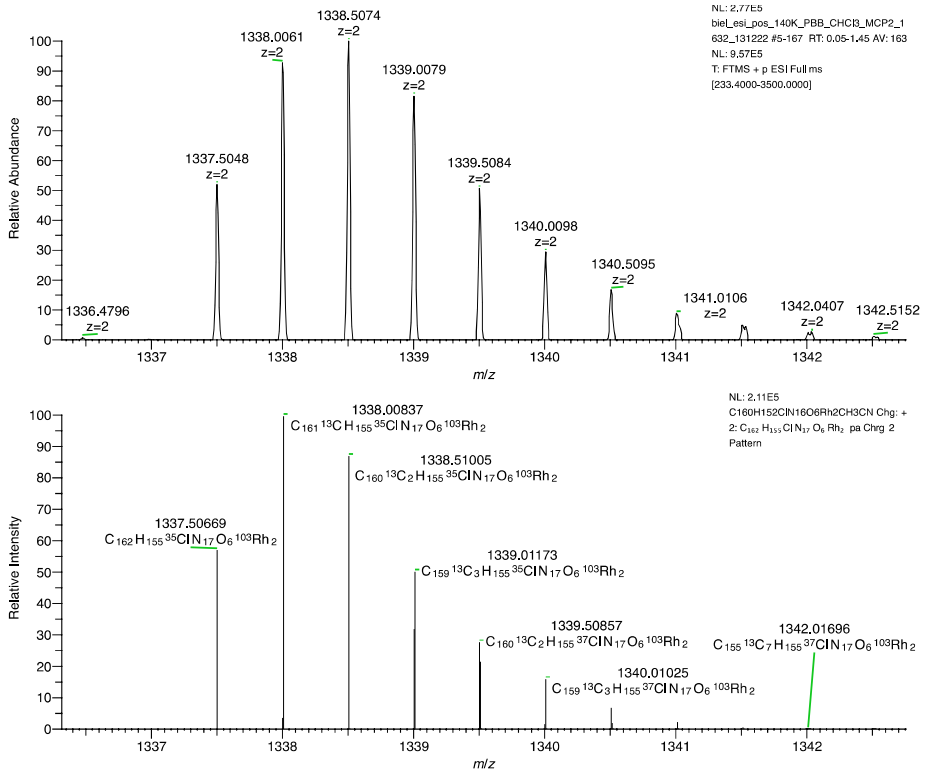

Figure S15. Experimental (top) and simulated (down) isotopic distribution of ion peak $[M\text{-}I+CH_3CN]^{2+}$ (M = **1-(RhI)(RhCl)•2**.

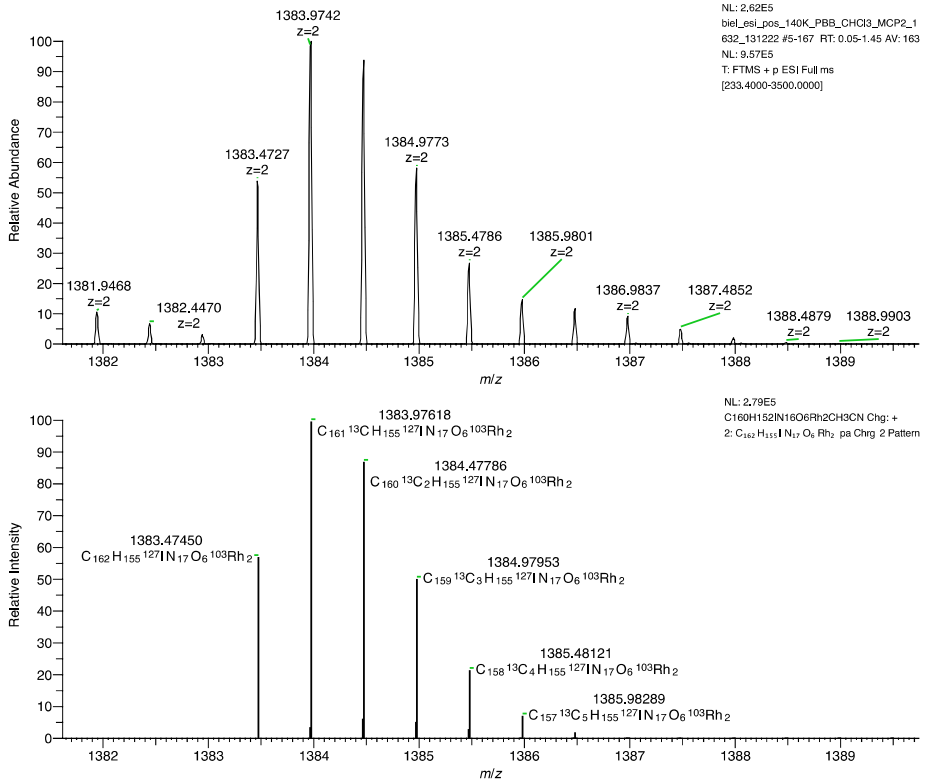

Figure S16. Experimental (top) and simulated (down) isotopic distribution of ion peak $[M\text{-}Cl+CH_3CN]^{2+}$ (M = **1-(RhI)(RhCl)•2**.

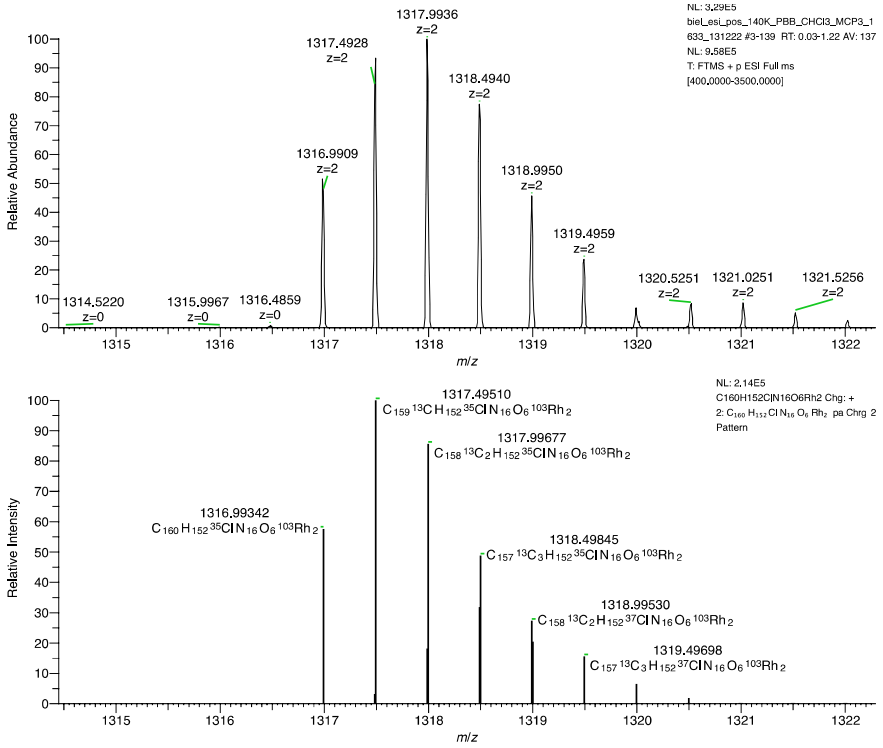

Figure S17. Experimental (top) and simulated (down) isotopic distribution of ion peak $[M\text{-}Cl]^{2+}$ (M = **1-(RhCl)$_2$•2**).

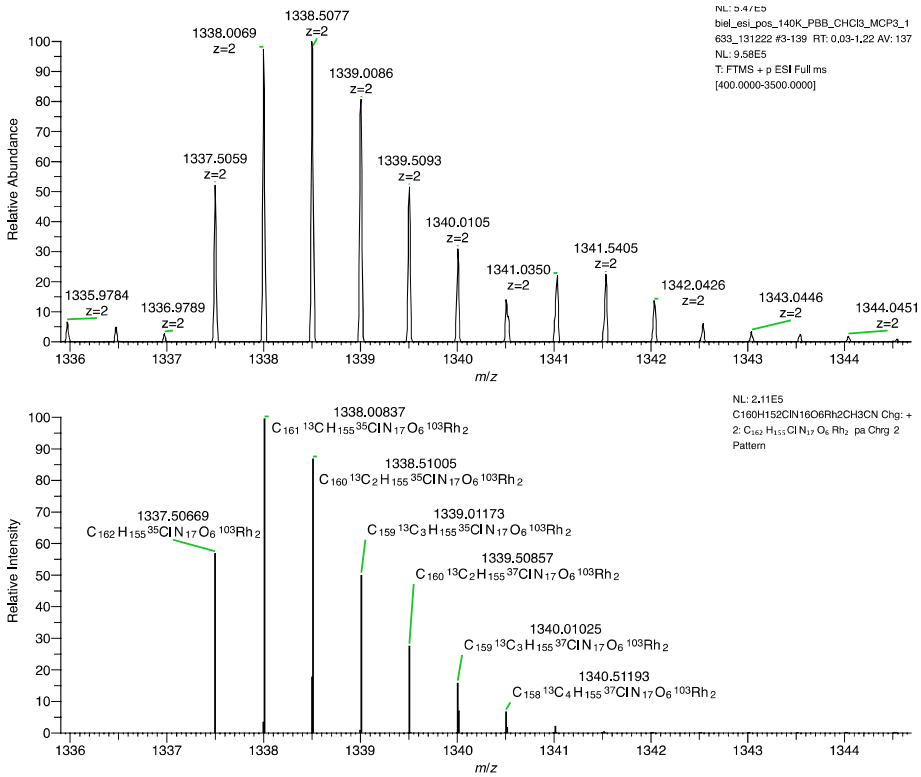

Figure S18. Experimental (top) and simulated (down) isotopic distribution of ion peak $[M\text{-}Cl+CH_3CN]^{2+}$ (M = **1-(RhCl)$_2$•2**).

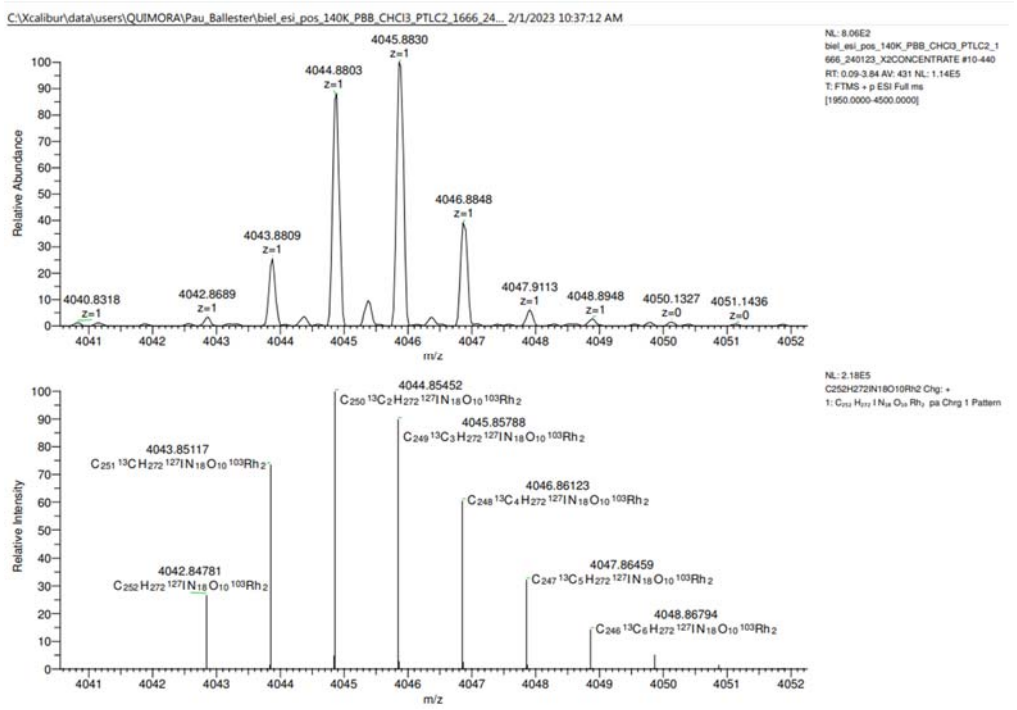

Figure S19. Experimental (top) and simulated (down) isotopic distribution of ion peak $[M\text{-}I]^+$ (M = **3b⊂[1-(RhI)$_2$•2]**).

5. ^{1}H NMR variable temperature studies

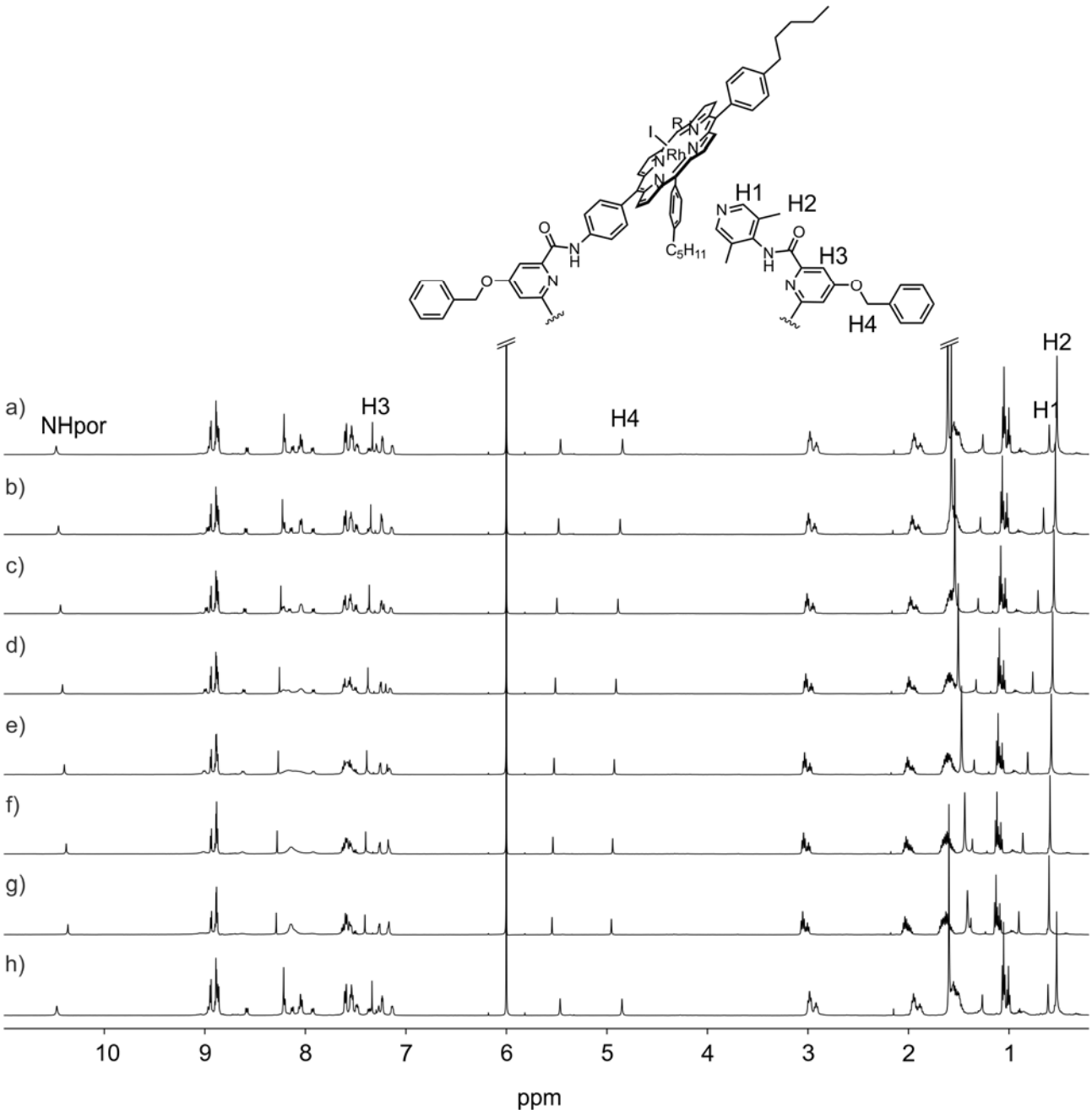

Figure S20. Variable temperature ^{1}H NMR spectra (500 MHz) of macrocycle **1-(RhI)$_2$•2** at (a) 293, (b) 313, (c) 333, (d) 353, (e) 373, (f) 393, (g) 413, and (h) 298 K in 1,1,2,2-tetrachloroethane-d_2. Spectrum (h) is after cooling down the solution from 413 K to 298 K.

6. Binding studies involving macrocycle 1-$(RhI)_2$•2 and adipamide 3a

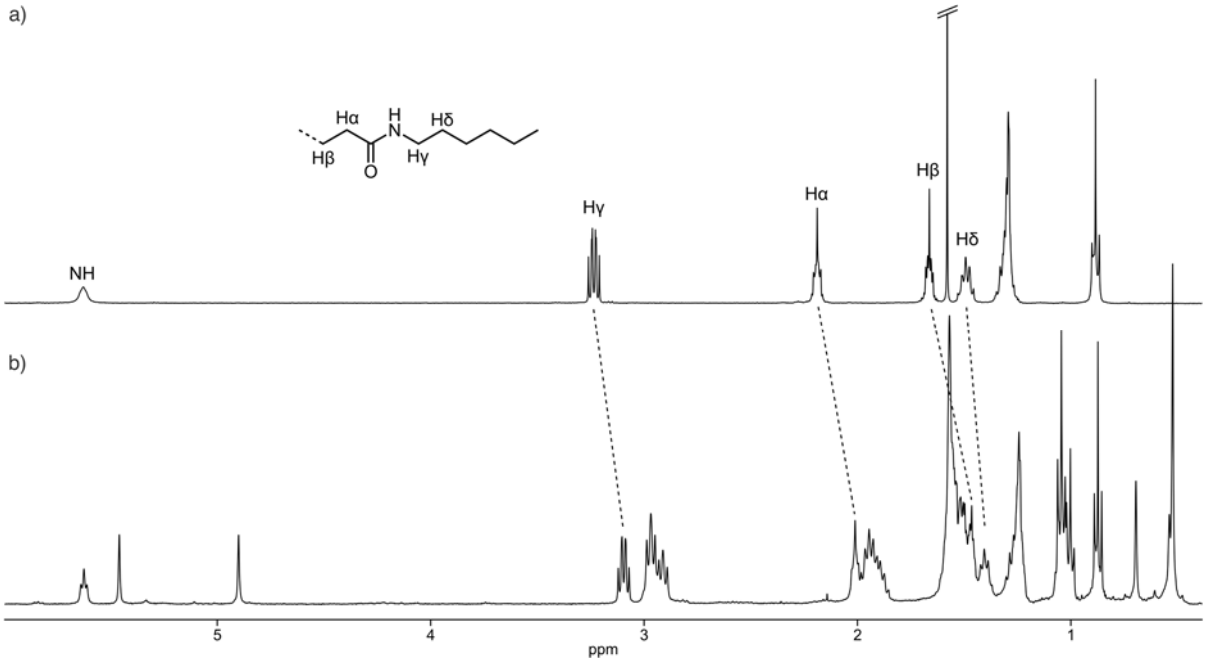

Figure S21. ^{1}H NMR spectra (400 MHz, 298 K) of (a) diamide **3a** (5.0×10^{-3} mol L^{-1}) and (b) a 1:1 mixture of **3a** and **1-$(RhI)_2$•2** in chloroform-*d*.

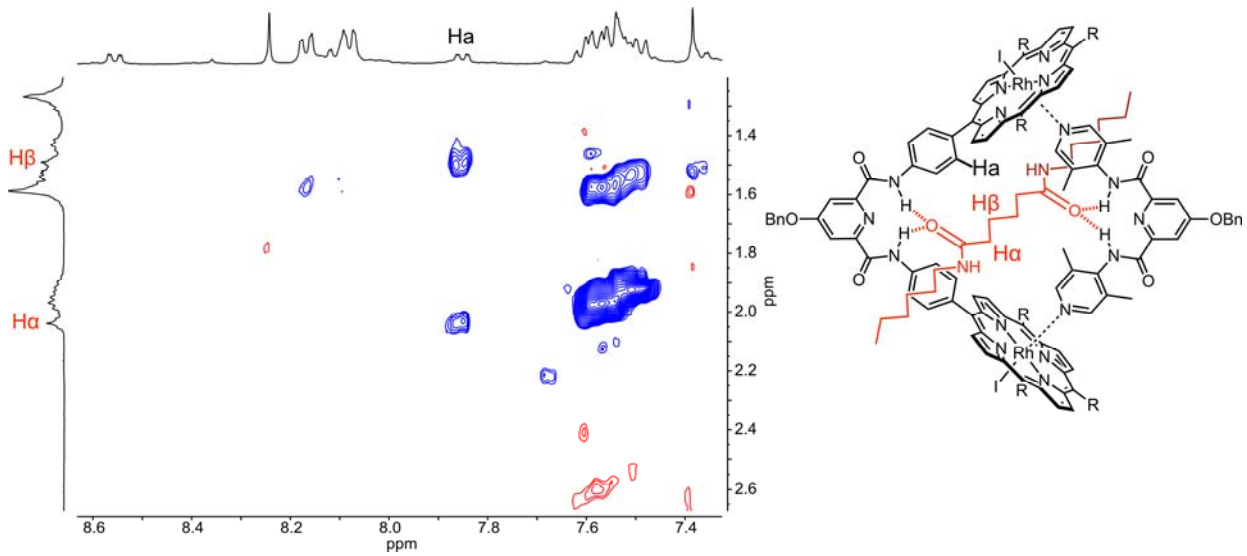

Figure S22. Selected region of the ROESY spectrum (400 MHz, 298 K) of a 1:1 mixture of **3a** and **1-$(RhI)_2$•2** in chloroform-*d*.

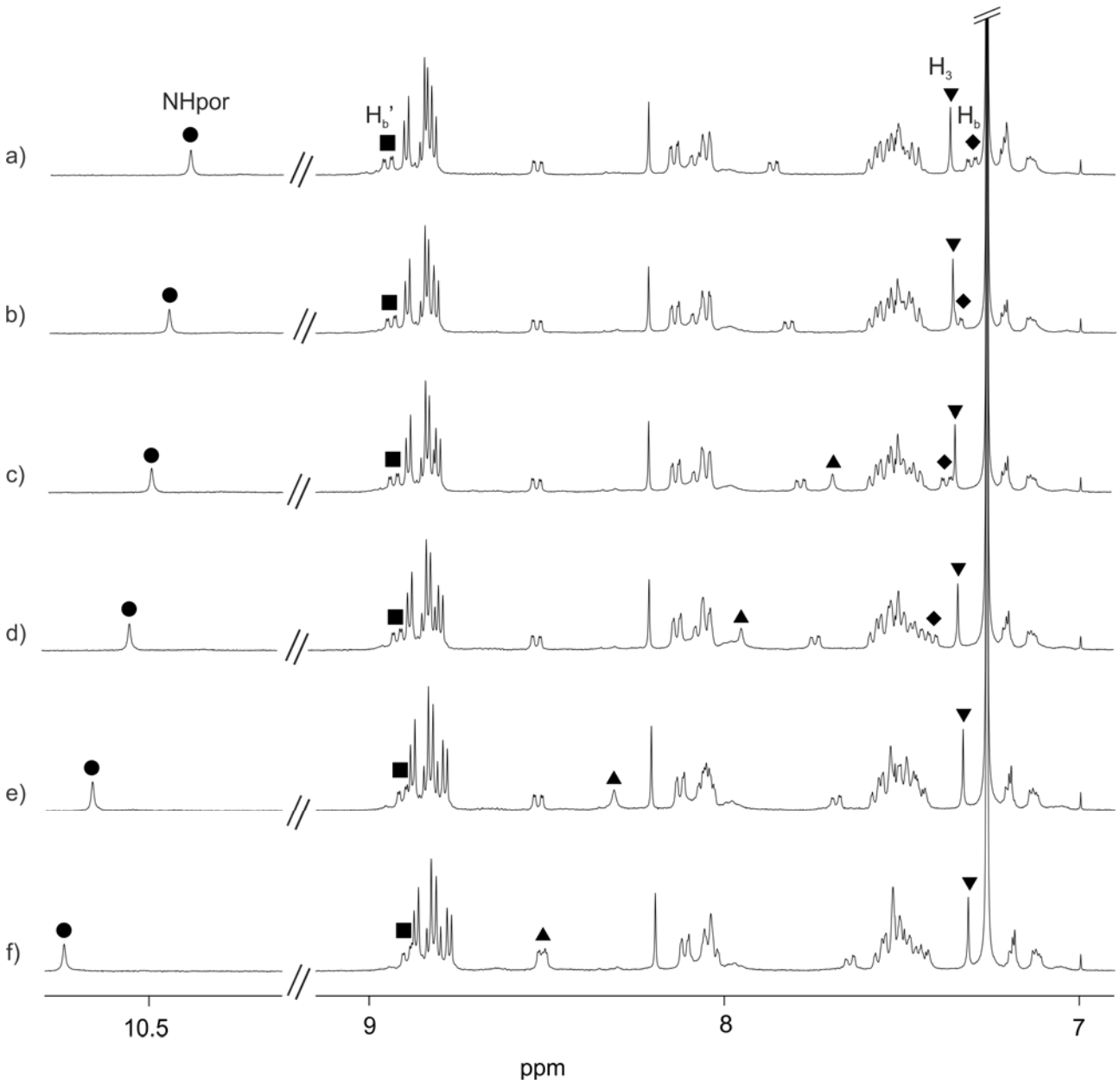

Figure S23. ^{1}H NMR spectra (400 MHz, 298 K) of macrocycle **1-(RhI)$_2$•2** (9.9×10^{-4} mol L^{-1}) upon addition of diamide **3a** in chloroform-*d*. (a) 0, (b) 4.7, (c) 9.9, (d) 20, (e) 51, (f) 102 equiv. of **3a**. For proton assignment see Figure S17.

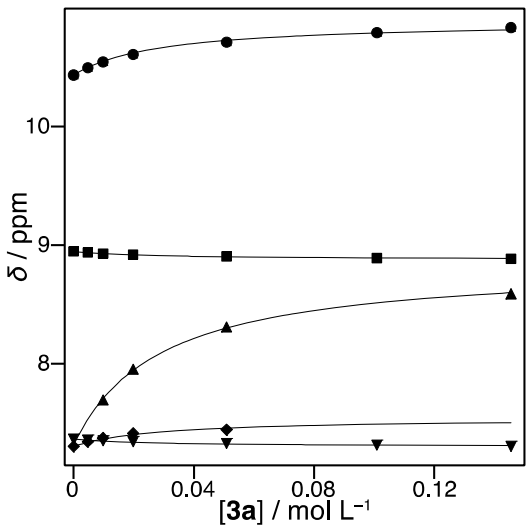

Figure S24. Chemical shift changes of selected proton signals of macrocycle **1-(RhI)$_2$•2** upon incremental additions of diamide **3a** (circles squares, triangles and diamonds) and fit of the titration data to a theoretical 1:1 model (solid line). K_{pseudo} = 36 M^{-1}. For proton assignment see Figure S20.

7. Binding studies involving macrocycle 1-$(RhI)_2$•2 and adipamide 3b

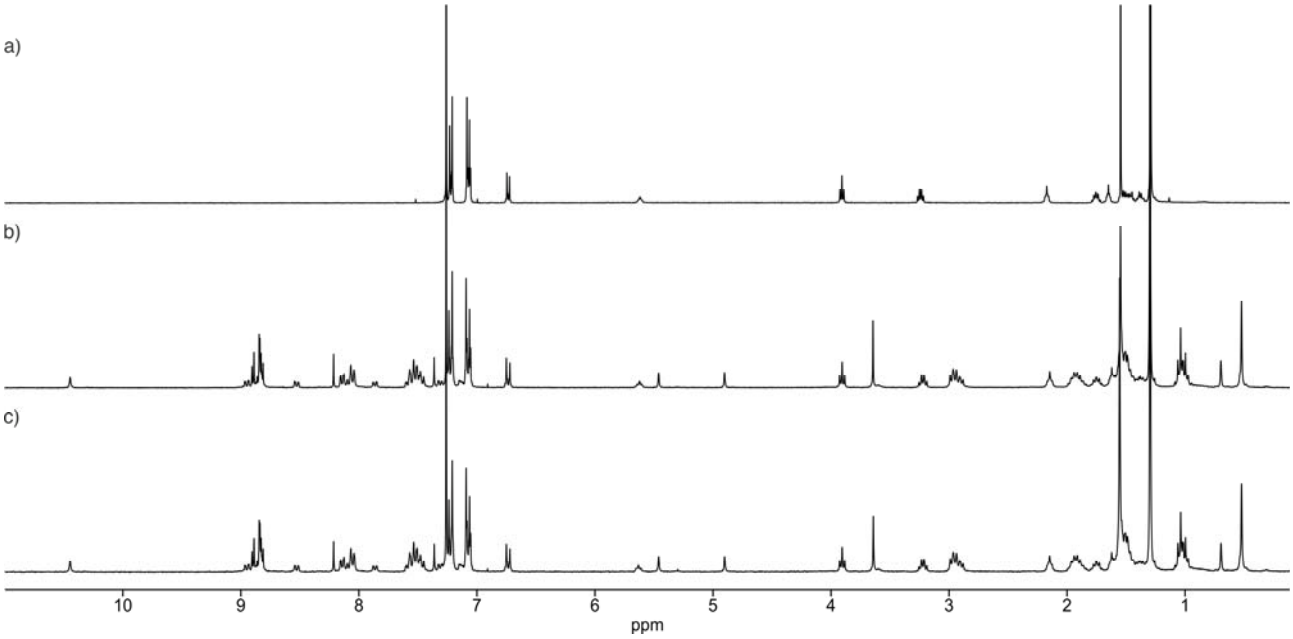

Figure S25. ^{1}H NMR spectra (300 MHz, 298 K) of (a) diamide **3b** (2.0×10^{-3} mol L^{-1}) and (b) a 1:1 mixture of **3b** and **1-$(RhI)_2$•2** in chloroform-*d*.

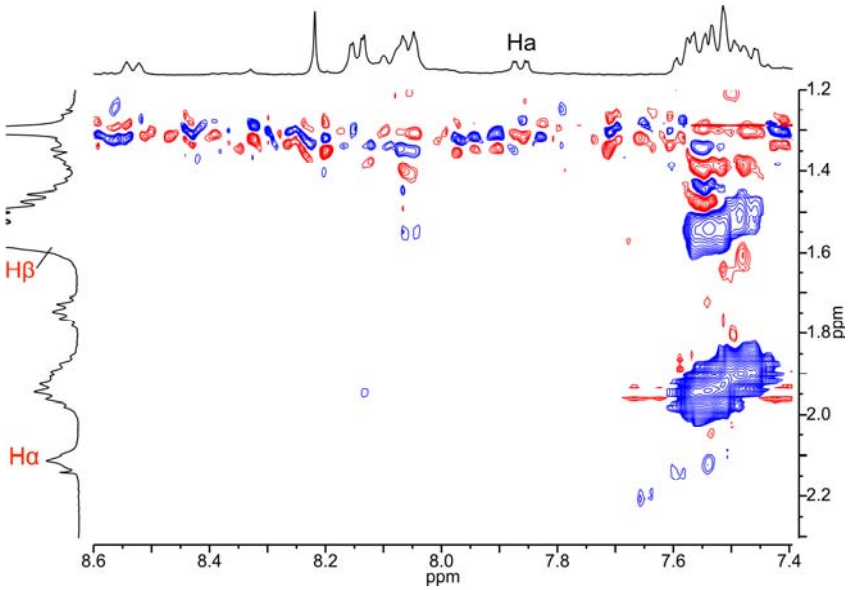

Figure S26. Selected region of the ROESY spectrum (400 MHz, 298 K) of a 1:1 mixture of **3b** and **1-$(RhI)_2$•2** in chloroform-*d*.

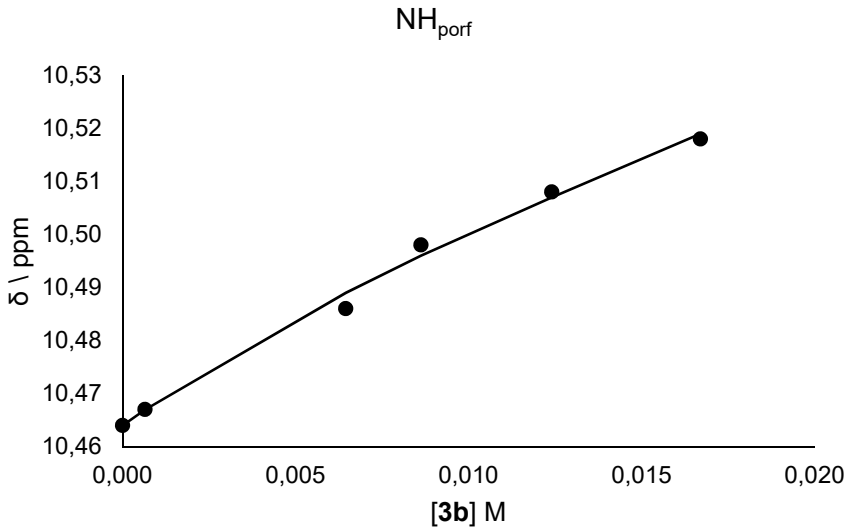

Figure S27. Chemical shift changes of the NH amide protons of the bis-porphyrin in macrocycle **1-(RhI)$_2$•2** upon incremental additions of diamide **3b** (circles) and fit of the titration data to a theoretical 1:1 model (solid line). K_{exo} = 18 M^{-1}.

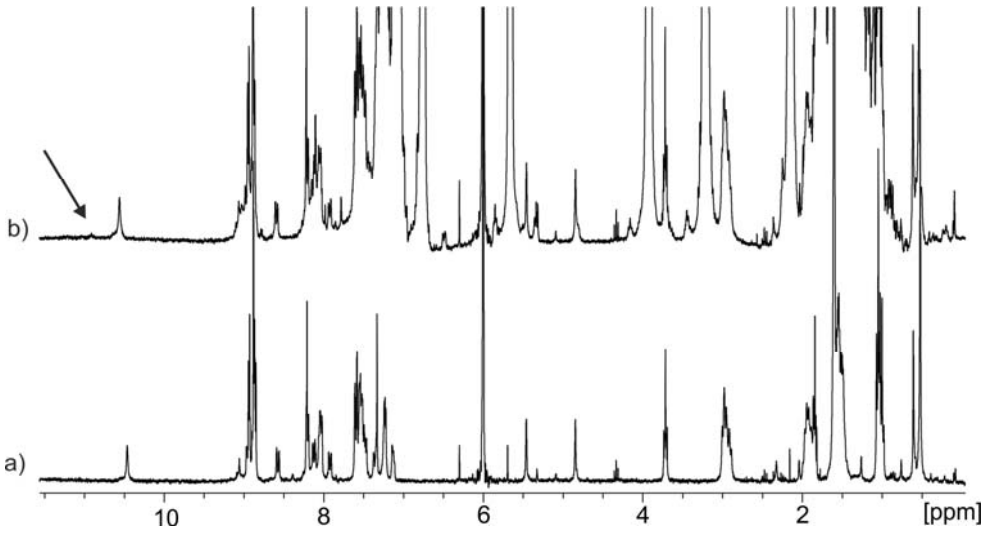

Figure S28. ^{1}H NMR spectra of a 1 mM solution of macrocycle **1-(RhI)$_2$•2** before (a) and after (b) the addition of 40 equiv. of **3b** and heating overnight to 80ºC.

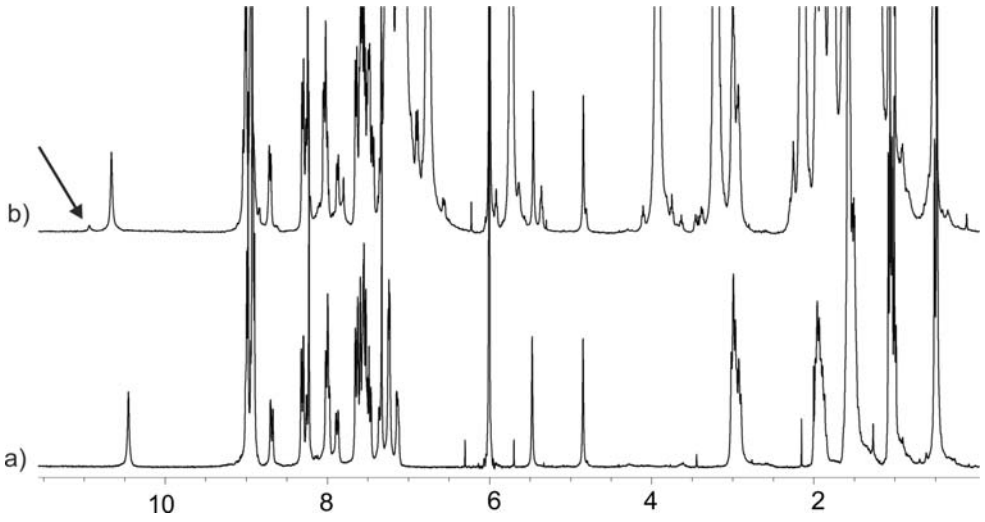

Figure S29. ^{1}H NMR spectra of a 4 mM solution of macrocycle **1-(RhCl)$_2$•2** before (a) and after (b) the addition of 15 equiv. of **3b** and heating overnight to 80ºC.

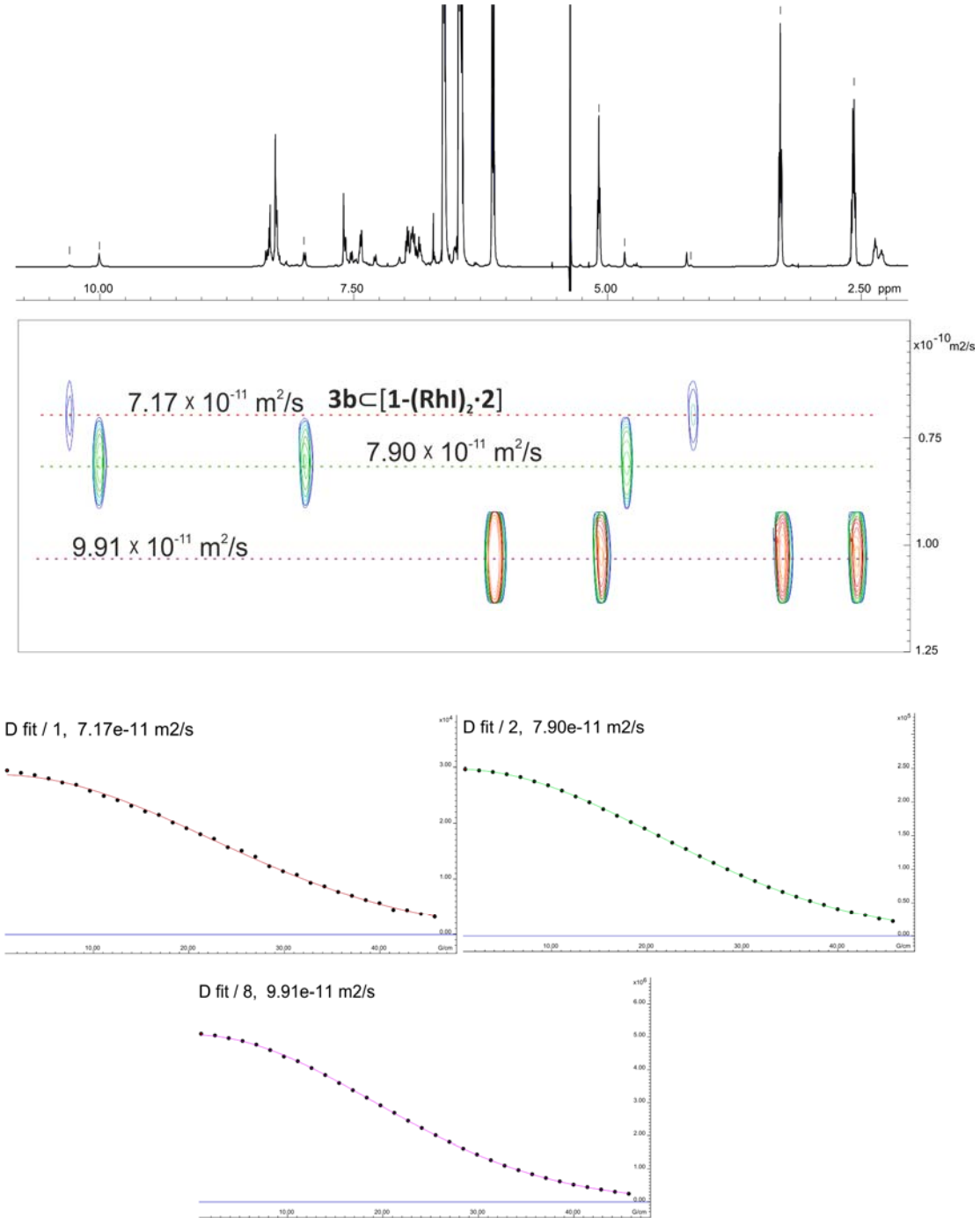

Figure S30. Top) Selected region of the ^{1}H pseudo-2D-plot of DOSY (500 MHz with cryoprobe, $(CDCl_2)_2$, 298 K, Δ = 150 ms, diffusion axis not shown in logarithmic scale). The selected peaks correspond to proton signals of the **3b⊂** [**1-(RhI)$_2$•2**] rotaxane (10.9 ppm), and to the macrocycle [**1-(RhI)$_2$•2**] (10.4 ppm) and lineal component **3b** (2.8 ppm). The latter two are involved in fast exchange on the DOSY timescale between free and bound states in the exo-complex **3b@**[**1-(RhI)$_2$•2**]. Bottom) Fits of the decays of a selected signal of each species to the mono-exponential Stejskal–Tanner function.

8. NMR characterization

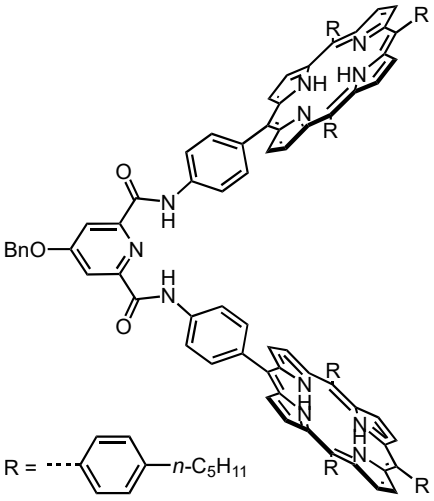

1-H₂

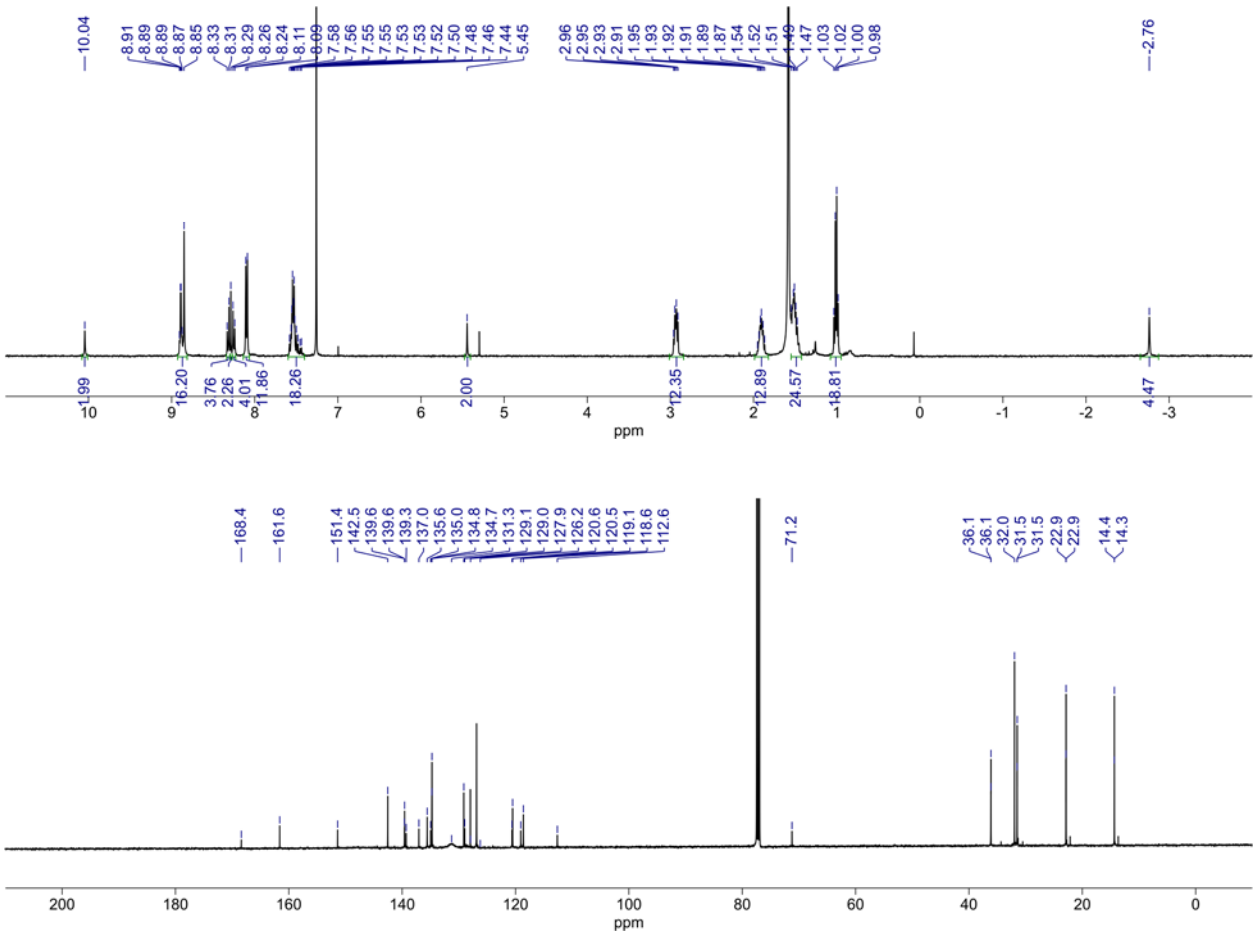

Figure S31. ^{1}H (400 MHz, 298 K) and ^{13}C{^{1}H} (125 MHz, 298 K) NMR spectra of **1-H₂** in chloroform-*d*.

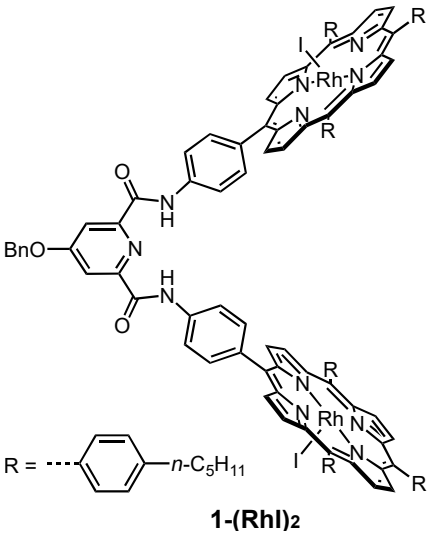

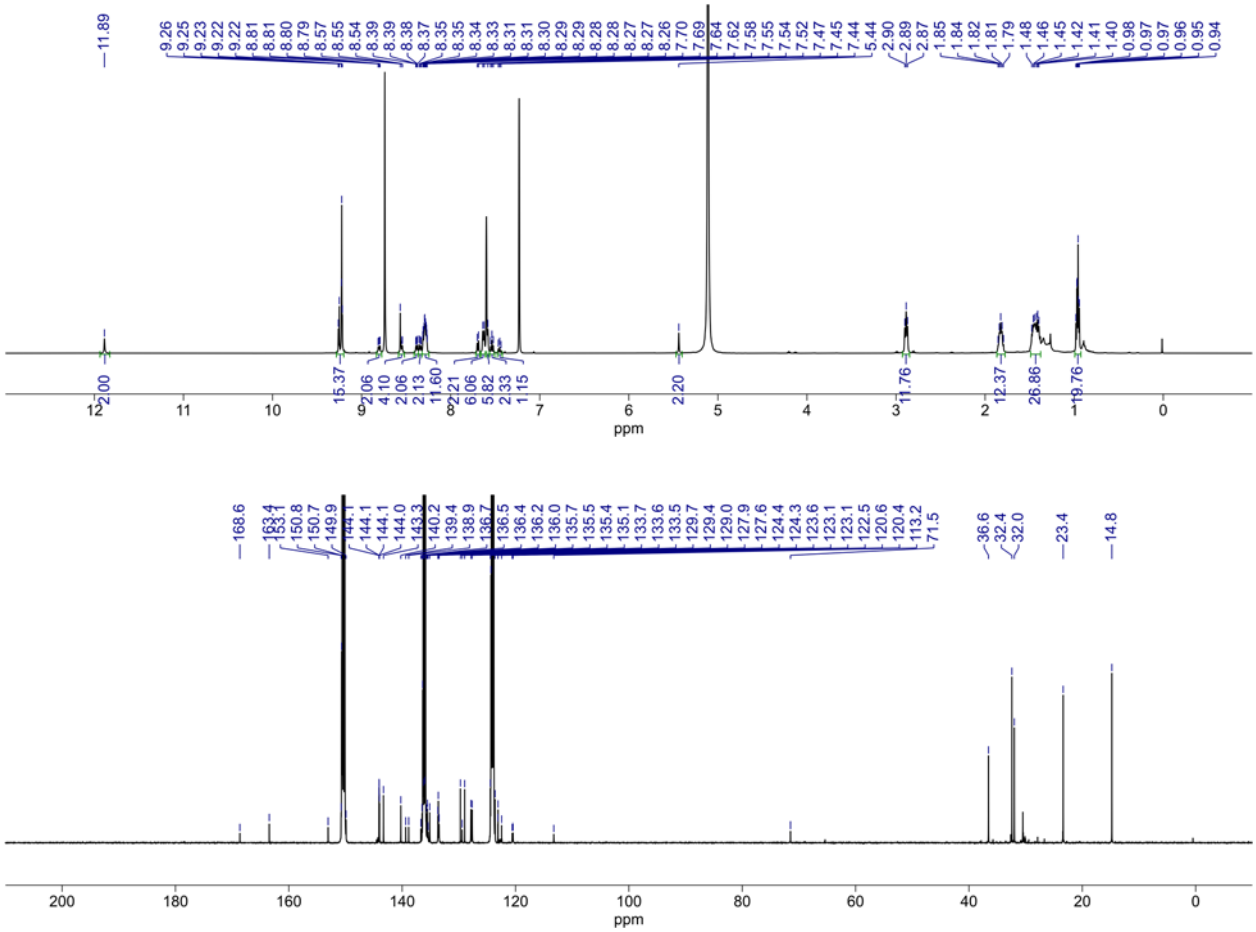

Figure S32. ^{1}H (400 MHz, 298 K) and ^{13}C{^{1}H} (125 MHz, 298 K) NMR spectra of **1-(RhI)$_2$** in pyridine-d_5.

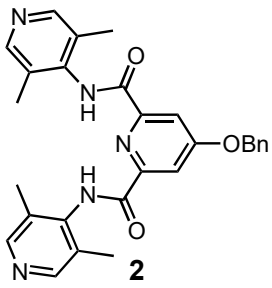

2

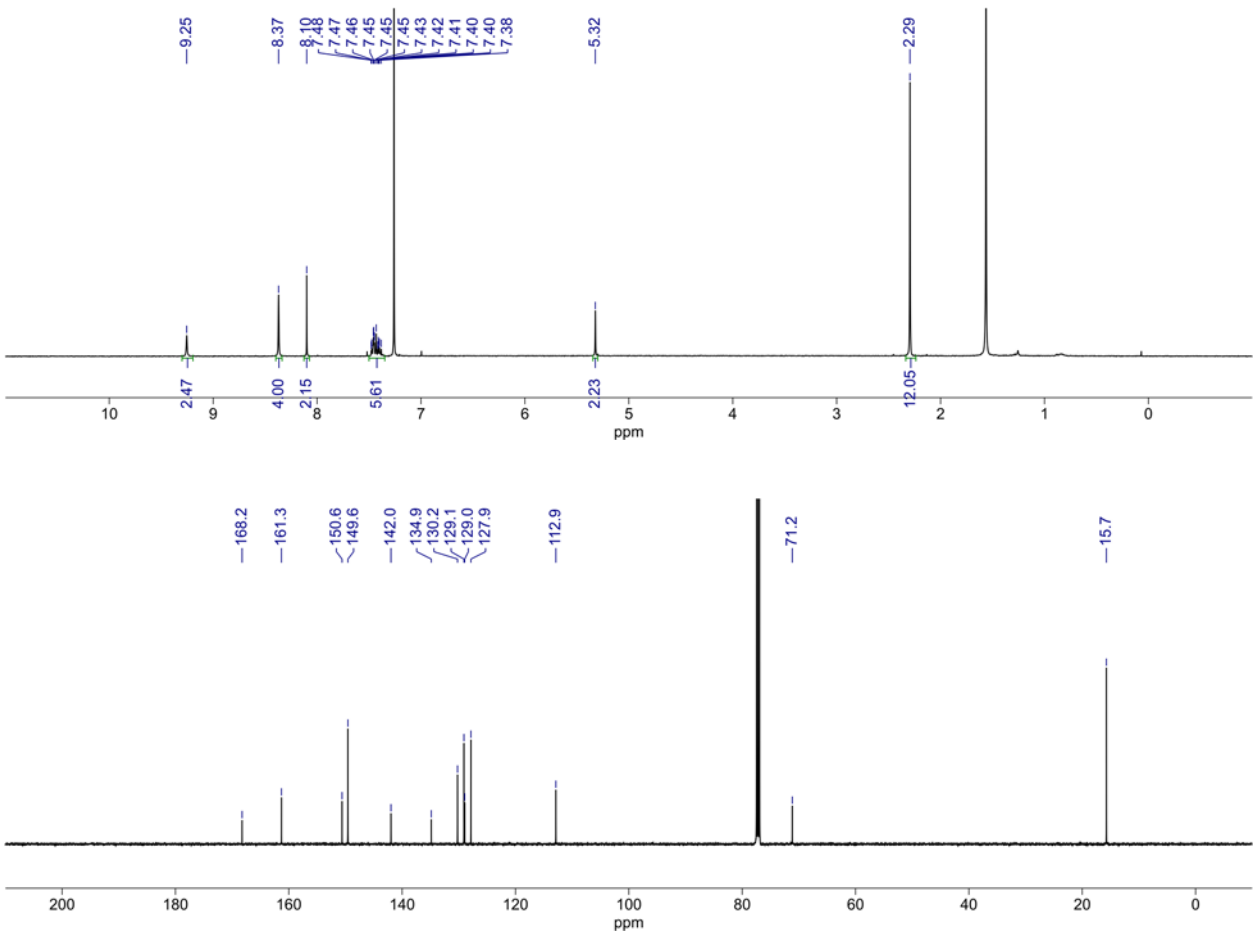

Figure S33. ^{1}H (400 MHz, 298 K) and $^{13}C\{^{1}H\}$ (125 MHz, 298 K) NMR spectra of **2** in chloroform-*d*.

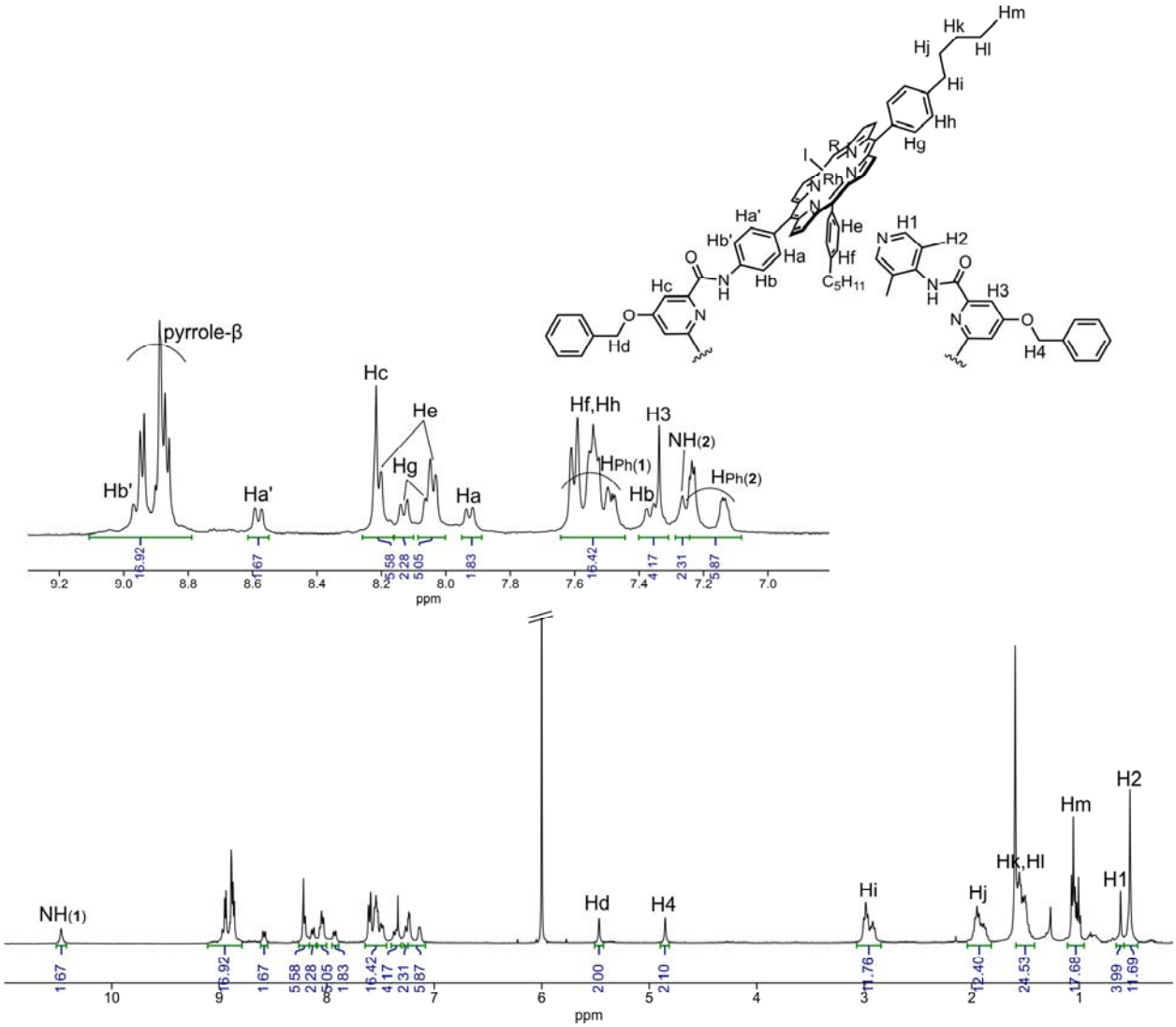

Figure S34. ^{1}H NMR spectrum (400 MHz, 298 K) of macrocycle **1-(RhI)$_2$•2** in 1,1,2,2-tetrachloroethane-d_2.

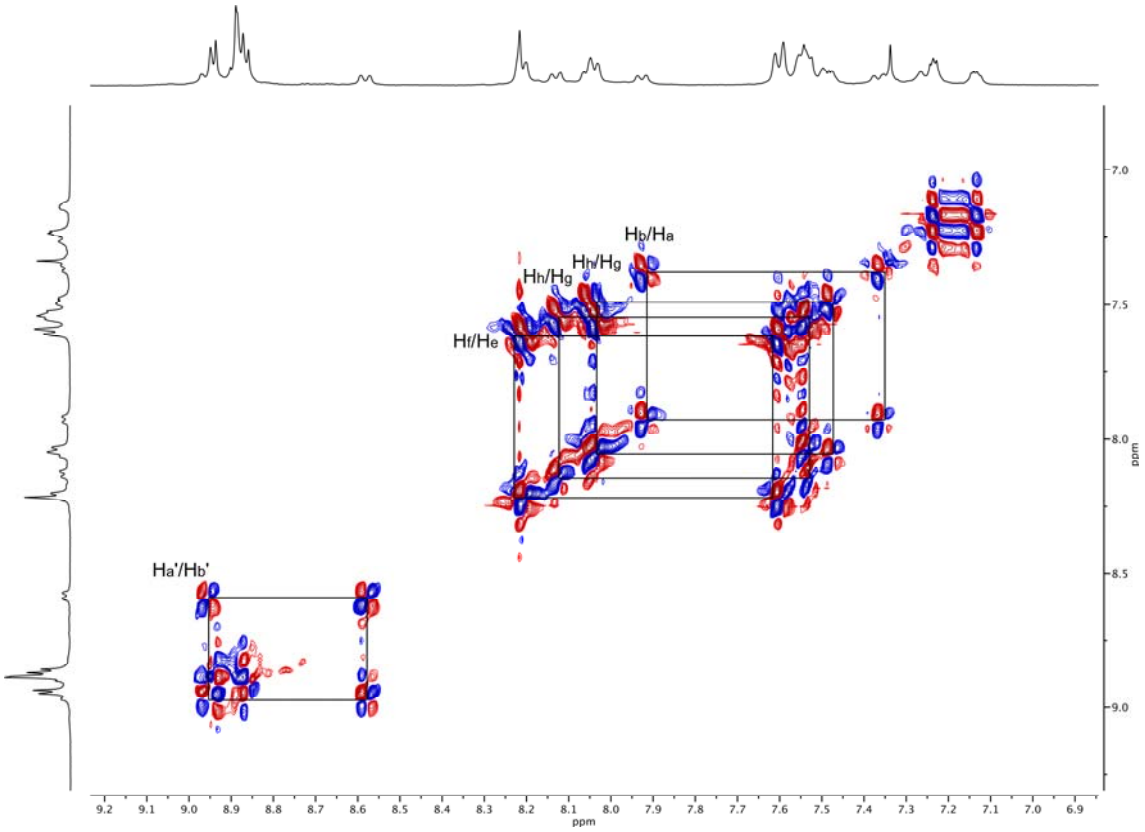

Figure S35. H-H COSY spectrum (400 MHz, 298 K) of macrocycle **1-(RhI)$_2$•2** in 1,1,2,2-tetrachloroethane-d_2.

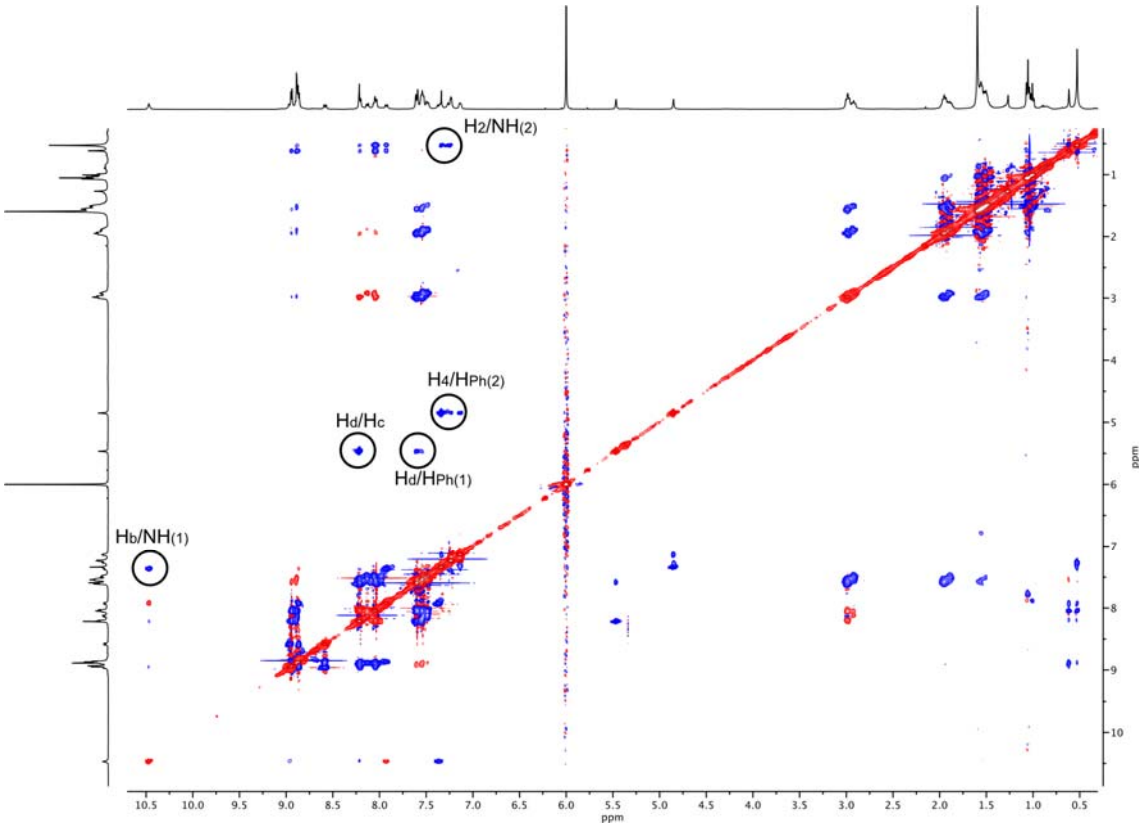

Figure S36. ROESY spectrum (400 MHz, 298 K) of macrocycle **1-(RhI)$_2$•2** in 1,1,2,2-tetrachloroethane-d_2.

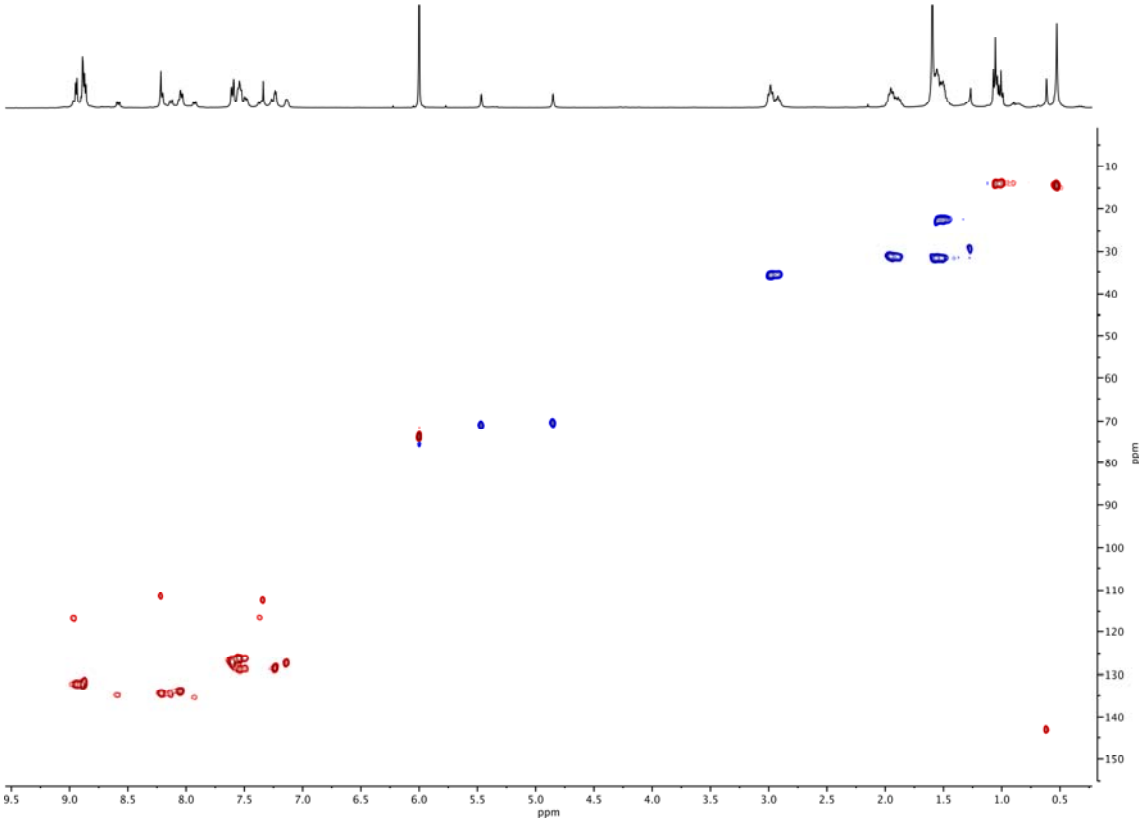

Figure S37. HSQC spectrum (400 MHz, 298 K) of macrocycle **1-(RhI)$_2$•2** in 1,1,2,2-tetrachloroethane-d_2.

9. References

(1) Chang, S.-Y.; Choi, J. S.; Jeong, K.-S., Self-Assembly and Dynamics of [2]- and [3]Rotaxanes with a Dinuclear Macrocycle Containing Reversible Os−N Coordinate Bonds. *Chem. Eur. J.* **2001**, *7*, 2687-2697.

(2) McKenzie, B. M.; Miller, A. K.; Wojtecki, R. J.; Johnson, J. C.; Burke, K. A.; Tzeng, K. A.; Mather, P. T.; Rowan, S. J., Improved synthesis of functionalized mesogenic 2,6-bisbenzimidazolylpyridine ligands. *Tetrahedron* **2008**, *64*, 8488-8495.

(3) Gardner, M.; J. Guerin, A.; A. Hunter, C.; Michelsen, U.; Rotger, C., Self-assembly of zinc aminoporphyrins. *New J. Chem.* **1999**, *23*, 309-316.

(4) Essery, J. M.; Schofield, K., Some derivatives of 4-amino- and 4-nitro-pyridine. *J. Chem. Soc.* **1960**, 4953-4959.